Electronic Research Archive

https://www.aimspress.com/journal/era

ERA, 34(7): 4410–4447.
DOI: 10.3934/era.2026195
Received: 30 January 2026
Revised: 20 April 2026
Accepted: 06 May 2026
Published: 22 May 2026

Research article

Modeling and optimal control of ADE-prone dual-strain influenza: balancing costs, risks, and interventions

Zongmin Yue*, **Yi Dong and Hui Cao**

School of Mathematics and Data Science, Shaanxi University of Science and Technology, Xi'an 710021, China

* **Correspondence:** Email: joanna_yzm@163.com.

Abstract: Antibody-dependent enhancement (ADE) is a major safety challenge in multiserotype disease control, involving complex trade-offs among infection burden, cost, and vaccine safety. This study develops a two-strain influenza model that integrates both host immunity (endogenous) and viral cross-reactivity (exogenous) as dual mechanisms underlying ADE. Threshold analysis shows that exogenous ADE lowers transmission thresholds ($\widetilde{R}_1$, $\widetilde{R}_A$), promoting strain coexistence, whereas endogenous ADE reverses this trend. We further establish a multiobjective optimal control framework to balance outbreak control, ADE risk, and intervention costs. The resulting strategy combines early targeted measures with sustained behavioral precautions (e.g., 51–79% mask-wearing compliance), effectively reducing the peak infection rate. Crucially, we identify an optimal risk-aversion level ($\alpha \approx 2$), which halves the ADE risk with only a 2.3% increase in infections and minimal extra cost—demonstrating a clear Pareto-optimal trade-off. This quantitative framework can be applied to other contexts, such as multivalent vaccine design for dengue fever, and provides a decision-making basis for risk-benefit assessment of vaccines against emerging infectious diseases.

Keywords: antibody-dependent enhancement (ADE); dual-strain influenza model; basic reproduction number; stability; optimal control

1. Introduction

Influenza is a highly contagious acute respiratory illness caused by influenza viruses of the family Orthomyxoviridae [1]. Influenza patients and asymptomatic carriers are the main source of influenza transmission [2]. Globally, influenza epidemics result in millions of deaths annually [3]. The Spanish influenza in 1918–1919 was the most devastating pandemic, causing approximately 40–50 million deaths [4–6]. The 1957–1958 Asian influenza pandemic resulted in an estimated 2 million fatalities, and the 1968–1969 Hong Kong influenza pandemic caused approximately 1 million deaths [4, 5].

During the 2023 spring peak in Fuzhou, China, monthly reported influenza cases reached 2749, marking the highest number reported in a single month over the past decade [7]. Influenza viruses are primarily classified into three types (A, B, and C), with Type A viruses further subdivided into subtypes based on differences in hemagglutinin (HA) and neuraminidase (NA), such as A/H1N1, A/H1N2, A/H3N2, and A/H5N1. Due to the rich dynamics of Influenza A subtypes and strains, Influenza A is also commonly used as a case study for multistrain pathogen modeling. It can be argued that the presence of multiple strains in populations increases the complexity of epidemic dynamics [8].

On the other hand, antibody-dependent enhancement (ADE) exerts non-negligible effects on the transmission dynamics of multistrain diseases. ADE constitutes a paradoxical phenomenon in host-pathogen biology, wherein antibodies, key pillars of the host's defense against pathogen invasion, actually facilitate pathogen entry into the host cells [9]. This rebellious behavior of antibodies further compromises the host's defense mechanisms, creating a microenvironment conducive to enhanced pathogen replication that exacerbates disease severity [9]. In fact, a wide range of diseases exhibit ADE both in vitro and/or in vivo, indicating that the effects of ADE can stem from both intrinsic (host-mediated) and extrinsic (pathogen-driven) influences. Extrinsic ADE effects are driven by heterologous viral cross-infection, whereas intrinsic ADE effects are mediated by host immune memory [10]. Diseases that have been confirmed to exhibit ADE include dengue virus, Zika virus, HIV, measles virus, and Influenza A virus, among others [11–15]. Gómez and Yang [11] developed a dengue virus model incorporating ADE to evaluate the impact of this phenomenon on heterologous dengue infections. Camargo et al. [12] simulated the dynamics of secondary infection induced by two distinct dengue virus serotypes under the competitive scenario between infection-neutralizing antibodies and infection-enhancing antibodies, and calculated the time at which maximum enhancement activity occurred. Billings et al. [13] discussed the effect of single-strain vaccine campaigns on the dynamics of epidemic multistrain models with ADE. Song et al. [14] established a SARS-CoV-2 infection dynamics model incorporating ADE to calculate the basic reproduction number and evaluate the potential impact of ADE on SARS-CoV-2 infection. The results demonstrated that ADE may accelerate SARS-CoV-2 infection. The researchers in [15] constructed a Zika-dengue coinfection model focusing on investigating the impact of ADE and dengue vaccination programs on disease control and prevention. However, few existing models have considered the impact of ADE on the transmission of multistrain influenza. References [9, 16] have explicitly indicated the potential existence of ADE in the context of influenza virus research. Thus, ADE represents an undeniable and critical factor in modeling the dissemination of multistrain influenza.

This study aims to construct a dynamic model of dual-strain influenza transmission under the influence of ADE. The model comprehensively integrates both endogenous and exogenous factors affecting disease transmission, with particular attention to the potential risks posed by asymptomatic individuals. Building upon this theoretical model, we conduct an empirical analysis of the 1918 influenza pandemic in Geneva, Switzerland, focusing on the effect of ADE on the final size of the epidemic. Furthermore, we apply a multiobjective Pareto optimization framework to influenza control strategies under ADE risk, quantifying the trade-off between infection control and safety by parameterizing the Pareto frontier with the risk-weighting coefficient α.

The structure of this paper is organized as follows. Section 2 presents the model formulation. Sections 3 and 4 provide the dynamic analysis, including the basic properties and stability of equilibria. Section 5 applies the model to empirically analyze the 1918 influenza pandemic in Geneva,

Switzerland. Based on practical considerations, Section 6 establishes a multiobjective optimal control model that accounts for ADE risks and analyzes the resulting optimal strategies. Finally, Section 7 provides concluding remarks.

2. Model development

The model workflow is illustrated in Figure 1. Generally, there are four main types of influenza viruses that circulate annually, but the primary causes of seasonal influenza in humans are two types: Influenza A and Influenza B. Influenza A viruses (e.g., H1N1, H3N2) are more likely to cause large-scale pandemics due to their high variability and broad host range, while Influenza B viruses (e.g., the Victoria/Yamagata lineages) typically lead to smaller-scale outbreaks [17]. The timing of influenza epidemic peaks may vary across different regions and years, and the peaks associated with different influenza virus strains may also differ. For example, Influenza A viruses (e.g., H1N1, H3N2) tend to cause large-scale epidemics and exhibit earlier peaks, whereas the peaks of Influenza B virus activity often occur later, sometimes following the peaks of Influenza A [18].

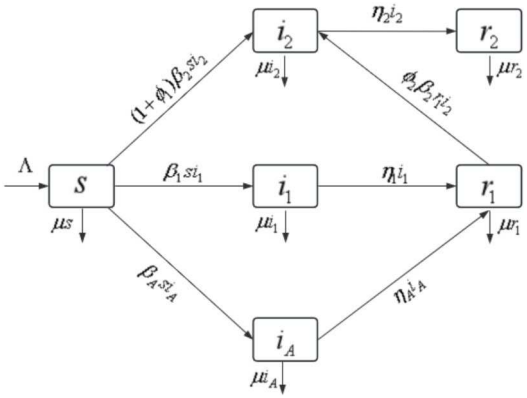

Figure 1. A flowchart of the model.

We assume two influenza strains: The initial infecting strain as the original strain, and the subsequent infecting strain as the new strain.

The population is divided into six compartments: The proportion of susceptible individuals (s), the proportion of symptomatic individuals infected by the original strain (i_1), the proportion of asymptomatic carriers infected by the original strain (i_A), the proportion recovered from infection by the original strain but susceptible to the new strain (r_1), the proportion of individuals infected by the new strain (i_2), and the proportion removed through recovery or treatment after infection with the new strain (r_2). The parameters used in the model are described in Table 1.

Since ADE is recognized as a complex phenomenon involving both exogenous and endogenous mechanisms that collectively enhance viral infectivity and replication [9], the ADE factor in the model acts on both the susceptible population s and the susceptible population r_1 that has recovered from the original strain. Its effect is manifested as enhancing the effective infection rate of the new strain on these two populations, with the respective intensities of the exogenous and endogenous effects distinguished by the parameters ϕ_1 and ϕ_2. Specifically, exogenous ADE (driven by heterologous viral cross-

infection) enhances the infection capability of the new strain on population s through parameter ϕ_1, while endogenous ADE (mediated by host immunological memory) enhances the infection capability of the new strain on population r_1 through parameter ϕ_2.

Table 1. Description of the model parameters.

Symbol	Description
β_1	Transmission rate of symptomatic individuals infected by the original strain
β_A	Transmission rate of asymptomatic carriers infected by the original strain
β_2	Transmission rate of individuals infected by the new strain
η_1	Recovery rate of symptomatic individuals infected by the original strain
η_A	Recovery rate of asymptomatic carriers infected by the original strain
η_2	Recovery rate of individuals infected by the new strain
μ	Natural death rate
Λ	Population recruitment rate
ϕ_1	Exogenous ADE-mediated enhancement factor for viral infectivity
ϕ_2	Endogenous ADE-mediated enhancement factor for viral infectivity

Under the foregoing assumptions, the following model is developed:

$$\begin{cases} \dfrac{ds}{dt} = \Lambda - \beta_1 s i_1 - \beta_A s i_A - (1+\phi_1)\beta_2 s i_2 - \mu s, \\ \dfrac{di_1}{dt} = \beta_1 s i_1 - (\eta_1 + \mu) i_1, \\ \dfrac{di_A}{dt} = \beta_A s i_A - (\eta_A + \mu) i_A, \\ \dfrac{dr_1}{dt} = \eta_1 i_1 + \eta_A i_A - \phi_2 \beta_2 r_1 i_2 - \mu r_1, \\ \dfrac{di_2}{dt} = (1+\phi_1)\beta_2 s i_2 + \phi_2 \beta_2 r_1 i_2 - \eta_2 i_2 - \mu i_2, \\ \dfrac{dr_2}{dt} = \eta_2 i_2 - \mu r_2. \end{cases} \tag{2.1}$$

Theorem 2.1. *The solution satisfying the initial conditions remains non-negative and bounded for all $t > 0$. Moreover, the set*

$$\Omega = \{(s(t), i_1(t), i_A(t), r_1(t), i_2(t), r_2(t)) \,\big|\, s(t), i_1(t), i_A(t), r_1(t), i_2(t), r_2(t) \geq 0, \\ 0 \leq s(t) + i_1(t) + i_A(t) + r_1(t) + i_2(t) + r_2(t) \leq \tfrac{\Lambda}{\mu}\}$$

is positively invariant under System (2.1).

Proof. If the total population is $N(t) = s(t) + i_1(t) + i_A(t) + r_1(t) + i_2(t) + r_2(t)$, then we get

$$\frac{dN}{dt} = \Lambda - \mu N.$$

It is easy to obtain

$$N(t) = \frac{\Lambda}{\mu} + e^{-\mu t}\left(N(0) - \frac{\Lambda}{\mu}\right).$$

Thus we have

$$\limsup_{t\to\infty} N(t) \le \frac{\Lambda}{\mu}.$$

Therefore, when $t \to \infty$, $0 \le N(t) \le \dfrac{\Lambda}{\mu}$ holds, i.e., Ω is the positive invariant set of System (2.1).

Since the equation for $\dfrac{dr_2}{dt}$ is actually decoupled from the other equations in System (2.1), we only need to consider the dynamics of the following five-dimensional subsystem (2.2):

$$\begin{cases} \dfrac{ds}{dt} = \Lambda - \beta_1 s i_1 - \beta_A s i_A - (1+\phi_1)\beta_2 s i_2 - \mu s, \\ \dfrac{di_1}{dt} = \beta_1 s i_1 - (\eta_1 + \mu) i_1, \\ \dfrac{di_A}{dt} = \beta_A s i_A - (\eta_A + \mu) i_A, \\ \dfrac{dr_1}{dt} = \eta_1 i_1 + \eta_A i_A - \phi_2\beta_2 r_1 i_2 - \mu r_1, \\ \dfrac{di_2}{dt} = (1+\phi_1)\beta_2 s i_2 + \phi_2\beta_2 r_1 i_2 - \eta_2 i_2 - \mu i_2. \end{cases} \tag{2.2}$$

3. Basic dynamic properties

3.1. Disease-free equilibrium and basic reproduction number

From the equations

$$\begin{cases} \Lambda - \beta_1 s i_1 - \beta_A s i_A - (1+\phi_1)\beta_2 s i_2 - \mu s = 0, \\ \beta_1 s i_1 - (\eta_1 + \mu) i_1 = 0, \\ \beta_A s i_A - (\eta_A + \mu) i_A = 0, \\ \eta_1 i_1 + \eta_A i_A - \phi_2\beta_2 r_1 i_2 - \mu r_1 = 0, \\ (1+\phi_1)\beta_2 s i_2 + \phi_2\beta_2 r_1 i_2 - \eta_2 i_2 - \mu i_2 = 0, \end{cases}$$

it is easy to obtain a disease-free equilibrium for System (2.2), namely $E_0 = \left(\frac{\Lambda}{\mu}, 0, 0, 0, 0\right)$. Next, we compute the basic reproduction number using the next-generation matrix method [19]. Let F and V be the matrices of the new infection terms and transition terms, respectively

$$F = \begin{pmatrix} \beta_1 s & 0 & 0 \\ 0 & \beta_A s & 0 \\ 0 & 0 & (1+\phi_1)\beta_2 s + \phi_2\beta_2 r_1 \end{pmatrix}, \quad V = \begin{pmatrix} \eta_1 + \mu & 0 & 0 \\ 0 & \eta_A + \mu & 0 \\ 0 & 0 & \eta_2 + \mu \end{pmatrix}.$$

It follows that

$$FV^{-1} = \begin{pmatrix} \dfrac{\beta_1 s}{\eta_1 + \mu} & 0 & 0 \\ 0 & \dfrac{\beta_A s}{\eta_A + \mu} & 0 \\ 0 & 0 & \dfrac{(1+\phi_1)\beta_2 s + \phi_2\beta_2 r_1}{\eta_2 + \mu} \end{pmatrix} = \begin{pmatrix} \dfrac{\beta_1}{\eta_1 + \mu}\dfrac{\Lambda}{\mu} & 0 & 0 \\ 0 & \dfrac{\beta_A}{\eta_A + \mu}\dfrac{\Lambda}{\mu} & 0 \\ 0 & 0 & \dfrac{(1+\phi_1)\beta_2}{\eta_2 + \mu}\dfrac{\Lambda}{\mu} \end{pmatrix}.$$

Thus, the basic reproduction number of System (2.2) is given by the spectral radius of the non-negative matrix, i.e.,

$$R_0 = \rho(FV^{-1}) = \max\left\{\frac{\beta_1}{\eta_1+\mu}\frac{\Lambda}{\mu}, \frac{\beta_A}{\eta_A+\mu}\frac{\Lambda}{\mu}, \frac{(1+\phi_1)\beta_2}{\eta_2+\mu}\frac{\Lambda}{\mu}\right\}.$$

We define

$$R_1 = \frac{\beta_1}{\eta_1+\mu}\frac{\Lambda}{\mu}, \quad R_A = \frac{\beta_A}{\eta_A+\mu}\frac{\Lambda}{\mu}, \quad R_2 = \frac{(1+\phi_1)\beta_2}{\eta_2+\mu}\frac{\Lambda}{\mu},$$

where R_1 denotes the reproduction number of symptomatic individuals infected by the original strain, R_A denotes the reproduction number of asymptomatic individuals infected by the original strain, and R_2 denotes the reproduction number of individuals infected by the new strain.

3.2. Stability of disease-free equilibrium

The Jacobian matrix of System (2.2) at the disease-free equilibrium E_0 is

$$J(E_0) = \begin{pmatrix} -\mu & -\beta_1\frac{\Lambda}{\mu} & -\beta_A\frac{\Lambda}{\mu} & 0 & -(1+\phi_1)\beta_2\frac{\Lambda}{\mu} \\ 0 & \beta_1\frac{\Lambda}{\mu}-(\eta_1+\mu) & 0 & 0 & 0 \\ 0 & 0 & \beta_A\frac{\Lambda}{\mu}-(\eta_A+\mu) & 0 & 0 \\ 0 & \eta_1 & \eta_A & -\mu & 0 \\ 0 & 0 & 0 & 0 & (1+\phi_1)\beta_2\frac{\Lambda}{\mu}-(\eta_2+\mu) \end{pmatrix}.$$

The corresponding characteristic equation is obtained as shown in Eq (3.1)

$$\frac{(\mu\lambda^2+2\mu^2\lambda+\mu^3)\left(-\lambda-\mu-\eta_1+\frac{\beta_1\Lambda}{\mu}\right)\left(-\lambda-\mu-\eta_A+\frac{\beta_A\Lambda}{\mu}\right)\left(-\lambda-\mu-\eta_2+\frac{(1+\phi_1)\beta_2\Lambda}{\mu}\right)}{\mu} = 0. \tag{3.1}$$

Thus the five eigenvalues can be found as follows:

$$\lambda_1 = \lambda_2 = -\mu,\ \lambda_3 = -\mu-\eta_1+\frac{\beta_1\Lambda}{\mu},\ \lambda_4 = -\mu-\eta_A+\frac{\beta_A\Lambda}{\mu},\ \lambda_5 = -\mu-\eta_2+\frac{(1+\phi_1)\beta_2\Lambda}{\mu}.$$

If $R_0 < 1$, we have $R_1 < 1, R_A < 1, R_2 < 1$, i.e., $\lambda_3 < 0, \lambda_4 < 0, \lambda_5 < 0$, and then all eigenvalues of $J(E_0)$ have negative real parts. When $R_1 > 1$ (or $R_A > 1$, or $R_2 > 1$), all eigenvalues of the Jacobian matrix $J(E_0)$ have at least one positive real part.

Consequently, System (2.2) is locally asymptotically stable at the disease-free equilibrium E_0 when $R_0 < 1$ and unstable at E_0 when $R_0 > 1$.

Next, we establish the global asymptotic stability of E_0.

Theorem 3.1. *The disease-free equilibrium E_0 of System* (2.2) *is globally asymptotically stable when $R_0 < 1$; E_0 becomes unstable when $R_0 > 1$.*

Proof. In fact, from the second and third equations of System (2.2), we can derive the following for $t \geq 0$:

$$i_1(t) = i_1(0)\exp\left(\int_0^t \beta_1 s(\tau)\,d\tau - (\eta_1+\mu)t\right), \tag{3.2}$$

$$i_A(t) = i_A(0)\exp\left(\int_0^t \beta_A s(\tau)\,d\tau - (\eta_A+\mu)t\right), \tag{3.3}$$

thus, for System (2.2), the $(n-2)$-dimensional subspace $\{s, i_1, i_A, r_1, i_2 \mid i_1 = 0,\ i_A = 0\}$ is invariant. From the first equation of System (2.2), it follows that $\frac{ds}{dt} \le \Lambda - \mu s$, thereby $s(t) \le \frac{\Lambda}{\mu}$. Thus combining (3.2) and (3.3), we have

$$i_1(t) \le i_1(0)e^{\int_0^t \beta_1 \frac{\Lambda}{\mu} d\tau - (\eta_1+\mu)t} = i_1(0)e^{\beta_1 \frac{\Lambda}{\mu} t - (\eta_1+\mu)t} = i_1(0)e^{(\eta_1+\mu)(R_1-1)t}.$$

Similarly, we obtain

$$i_A(t) \le i_A(0)e^{(\eta_A+\mu)(R_A-1)t}.$$

If $R_0 < 1$, then $R_1 - 1 < 0$, $R_A - 1 < 0$, and therefore $i_1(t) \xrightarrow{t\to\infty} 0$, $i_A(t) \xrightarrow{t\to\infty} 0$. Subsequently, to demonstrate the global asymptotic stability of E_0 on the $(n-2)$-dimensional subspace $\{s, i_1, i_A, r_1, i_2 \mid i_1 = 0,\ i_A = 0\}$, we construct a classical Lyapunov function leveraging the properties of the function $f(x) = x - 1 - \ln(x)$. Let

$$V(s, r_1, i_2) = s_0\left(\frac{s}{s_0} - 1 - \ln\frac{s}{s_0}\right) + r_1 + i_2.$$

Along the trajectories of System (2.2) in the $(n-2)$-dimensional subspace $\{s, i_1, i_A, r_1, i_2 \mid i_1 = 0,\ i_A = 0\}$, we obtain

$$\begin{aligned}
\frac{dV}{dt} &= \frac{ds}{dt}\left(1 - \frac{s_0}{s}\right) + \frac{dr_1}{dt} + \frac{di_2}{dt} \\
&= \left(1 - \frac{s_0}{s}\right)(\Lambda - (1+\phi_1)\beta_2 s i_2 - \mu s) - \phi_2\beta_2 r_1 i_2 - \mu r_1 + (1+\phi_1)\beta_2 s i_2 + \phi_2\beta_2 r_1 i_2 - \eta_2 i_2 - \mu i_2 \\
&= \Lambda - (1+\phi_1)\beta_2 s i_2 - \mu s - \frac{s_0}{s}\Lambda + (1+\phi_1)\beta_2 s_0 i_2 + \mu s_0 - \phi_2\beta_2 r_1 i_2 \\
&\quad - \mu r_1 + (1+\phi_1)\beta_2 s i_2 + \phi_2\beta_2 r_1 i_2 - \eta_2 i_2 - \mu i_2 \\
&= \mu s_0\left(2 - \frac{s}{s_0} - \frac{s_0}{s}\right) + i_2((1+\phi_1)\beta_2 s_0 - \eta_2 - \mu) - \mu r_1 \\
&= \mu s_0\left(2 - \frac{s}{s_0} - \frac{s_0}{s}\right) + i_2(\eta_2+\mu)(R_2 - 1) - \mu r_1.
\end{aligned}$$

If $R_0 < 1$, then $R_2 - 1 < 0$. Moreover, by the inequality of the arithmetic and geometric means, we obtain $\frac{dV}{dt} \le 0$. Therefore, Lyapunov stability theory guarantees that E_0 is globally asymptotically stable.

3.3. The existence of equilibria

Remark 3.1. *For clarity in representing the existence and stability conditions, we let*

$$\widetilde{R}_1 = \frac{\beta_1\Lambda}{\mu\left(\mu + \eta_1 + \eta_1(R_1 - 1)\frac{\phi_2}{(1+\phi_1)}\right)}, \quad \widetilde{R}_A = \frac{\beta_A\Lambda}{\mu\left(\mu + \eta_A + \eta_A(R_A - 1)\frac{\phi_2}{(1+\phi_1)}\right)}.$$

Clearly, if $R_1 > 1$, *then* $R_1 > \widetilde{R}_1$; *if* $R_1 < 1$, *then* $R_1 < \widetilde{R}_1$.
Analogously, if $R_A > 1$, *then* $R_A > \widetilde{R}_A$; *if* $R_A < 1$, *then* $R_A < \widetilde{R}_A$.

Let

$$\widetilde{\widetilde{R}}_1 = \frac{\eta_1 + \mu}{\mu} R_1, \quad \widetilde{\widetilde{R}}_A = \frac{\eta_A + \mu}{\mu} R_A.$$

Obviously, $R_1 < \widetilde{\widetilde{R}}_1$, $R_A < \widetilde{\widetilde{R}}_A$.

Theorem 3.2. *For System* (2.2)*, the following statements hold.*
1) The boundary equilibrium $E_1(s_1, i_{11}, 0, r_{11}, 0)$ *exists if and only if* $R_1 > 1$.
2) The boundary equilibrium $E_A(s_A, 0, i_{AA}, r_{1A}, 0)$ *exists if and only if* $R_A > 1$.
3) The boundary equilibrium $E_2(s_2, 0, 0, 0, i_{22})$ *exists if and only if* $R_2 > 1$.
4) The endemic equilibrium $\bar{E}(\bar{s}, \bar{i}_1, 0, \bar{r}_1, \bar{i}_2)$ *exists if and only if* $\widetilde{R}_1 < R_2 < R_1$.
5) The endemic equilibrium $\hat{E}(\hat{s}, 0, \hat{i}_A, \hat{r}_1, \hat{i}_2)$ *exists if and only if* $\widetilde{R}_A < R_2 < R_A$.

Proof. In System (2.2), the boundary equilibria E_1, E_A, and E_2 represent scenarios where only one disease state exists: $E_1(s_1, i_{11}, 0, r_{11}, 0)$ corresponds to the boundary equilibrium with only symptomatic individuals infected by the original strain, $E_A(s_A, 0, i_{AA}, r_{1A}, 0)$ represents the boundary equilibrium with only asymptomatic individuals infected by the original strain, and $E_2(s_2, 0, 0, 0, i_{22})$ denotes the boundary equilibrium with susceptible individuals infected solely by the new strain.

At the boundary equilibrium $E_1(s_1, i_{11}, 0, r_{11}, 0)$, we have

$$s_1 = \frac{\eta_1 + \mu}{\beta_1}, \quad i_{11} = \frac{\Lambda}{\eta_1 + \mu} - \frac{\mu}{\beta_1} = \frac{\mu}{\beta_1}(R_1 - 1), \quad r_{11} = \frac{\eta_1 \Lambda}{\mu(\eta_1 + \mu)} - \frac{\eta_1}{\beta_1} = \frac{\eta_1}{\beta_1}(R_1 - 1).$$

Clearly, E_1 is biologically meaningful if and only if $R_1 - 1 > 0$, that is, the boundary equilibrium E_1 exists if and only if $R_1 > 1$.

Similarly, for the boundary equilibrium $E_A(s_A, 0, i_{AA}, r_{1A}, 0)$, we have

$$s_A = \frac{\eta_A + \mu}{\beta_A}, \quad i_{AA} = -\frac{(\eta_A \mu - \beta_A \Lambda + \mu^2)}{\beta_A(\eta_A + \mu)} = \frac{\mu}{\beta_A}(R_A - 1), \quad r_{1A} = -\frac{\eta_A(\eta_A \mu - \beta_A \Lambda + \mu^2)}{\beta_A \mu(\eta_A + \mu)} = \frac{\eta_A}{\beta_A}(R_A - 1).$$

It is clear that the boundary equilibrium E_A exists if and only if $R_A > 1$.

For the boundary equilibrium $E_2(s_2, 0, 0, 0, i_{22})$, we have

$$s_2 = \frac{\eta_2 + \mu}{(1 + \phi_1)\beta_2}, \quad i_{22} = -\frac{(\eta_2 \mu + \mu^2 - \beta_2 \Lambda(1 + \phi_1))}{\beta_2 \eta_2 (1 + \phi_1) + \beta_2 \mu (1 + \phi_1)} = \frac{\Lambda}{\eta_2 + \mu} - \frac{\mu}{\beta_2(1 + \phi_1)} = \frac{\mu}{(1 + \phi_1)\beta_2}(R_2 - 1).$$

It follows that E_2 exists if and only if $R_2 > 1$.

In System (2.2), the endemic equilibria $\bar{E}$ and $\hat{E}$ represent two distinct coexistence scenarios: $\bar{E}(\bar{s}, \bar{i}_1, 0, \bar{r}_1, \bar{i}_2)$ characterizes the coexistence of both original-strain-induced symptomatic infections and new-strain-induced symptomatic cases, while $\hat{E}(\hat{s}, 0, \hat{i}_A, \hat{r}_1, \hat{i}_2)$ corresponds to the coexistence of original-strain-asymptomatic carriers and new-strain-symptomatic infections.

Consider the endemic equilibrium $\bar{E}(\bar{s}, \bar{i}_1, 0, \bar{r}_1, \bar{i}_2)$, where

$$\bar{s} = \frac{\eta_1 + \mu}{\beta_1} = \frac{\Lambda}{\mu} \frac{1}{R_1},$$

$$\bar{r}_1 = \frac{\eta_2+\mu}{\phi_2\beta_2} - \frac{(1+\phi_1)(\eta_1+\mu)}{\phi_2\beta_1} = \frac{(1+\phi_1)}{\phi_2}\frac{\Lambda}{\mu}(\frac{1}{R_2} - \frac{1}{R_1}),$$
$$\bar{i}_1 = \frac{(\beta_1(\eta_2+\mu) - \beta_2(1+\phi_1)(\eta_1+\mu))f}{\phi_2\beta_1(\eta_1+\mu)(\beta_1(\eta_2+\mu) - (1+\phi_1)\beta_2\mu)} = \frac{\mu(R_1-R_2)f}{\phi_2\beta_1(\Lambda\beta_1 - \mu^2R_2)},$$
$$\bar{i}_2 = \frac{\Lambda\beta_1\eta_1}{(\eta_1+\mu)(\beta_1(\eta_2+\mu) - (1+\phi_1)\beta_2\mu)} - \frac{\mu(\beta_1(\eta_2+\mu) - (1+\phi_1)\beta_2\mu - ((1+\phi_1)-\phi_2)\beta_2\eta_1)}{\phi_2\beta_2(\beta_1(\eta_2+\mu) - (1+\phi_1)\beta_2\mu)},$$

where

$$f = ((1+\phi_1)-\phi_2)\mu(\eta_1+\mu) + \phi_2\beta_1\Lambda.$$

Clearly, to ensure biological significance of $\bar{E}$, the conditions $\bar{r}_1 > 0$, $\bar{i}_1 > 0$, and $\bar{i}_2 > 0$ must hold. The following discusses if $\bar{r}_1 > 0$, which is equivalent to

$$\frac{\eta_2+\mu}{\phi_2\beta_2} > \frac{(1+\phi_1)(\eta_1+\mu)}{\phi_2\beta_1} \quad \Leftrightarrow \quad R_2 < R_1. \tag{3.4}$$

For $\bar{i}_1 > 0$ to hold, the following two cases may occur:
Case 1. $\Lambda\beta_1 - \mu^2R_2 > 0$ and $f > 0$;
Case 2. $\Lambda\beta_1 - \mu^2R_2 < 0$ and $f < 0$.
By combining (3.4) with the non-negativity analysis of parameter η_1, it can be concluded that Case 2 contradicts Condition (3.4). This is because if $\Lambda\beta_1 - \mu^2R_2 < 0$ holds, then $R_2 > \frac{\Lambda\beta_1}{\mu^2}$, which clearly contradicts $R_2 < \frac{\Lambda\beta_1}{\mu(\eta_1+\mu)}$. Therefore, only Case 1 is valid. In other words, if $\bar{i}_1 > 0$, it is equivalent to

$$R_2 < \frac{\Lambda\beta_1}{\mu^2}, \tag{3.5}$$

and

$$\frac{(1+\phi_1)}{\phi_2} > 1 - R_1. \tag{3.6}$$

Finally, the condition for $\bar{i}_2 > 0$ to hold is equivalent to

$$\begin{aligned}
&\frac{\Lambda\beta_1\eta_1}{(\eta_1+\mu)(\beta_1(\eta_2+\mu) - (1+\phi_1)\beta_2\mu)} > \frac{\mu(\beta_1(\eta_2+\mu) - (1+\phi_1)\beta_2\mu - ((1+\phi_1)-\phi_2)\beta_2\eta_1)}{\phi_2\beta_2(\beta_1(\eta_2+\mu) - (1+\phi_1)\beta_2\mu)},\\
\Leftrightarrow\ &\frac{1}{\eta_1+\mu} > \frac{(1+\phi_1)}{\phi_2\eta_1}\frac{1}{R_2} - \frac{(1+\phi_1)\mu}{\phi_2\eta_1(\eta_1+\mu)}\frac{1}{R_1} - \frac{((1+\phi_1)-\phi_2)\mu}{\phi_2\beta_1\Lambda},\\
\Leftrightarrow\ &\frac{1}{R_2} < \frac{\phi_2\eta_1R_1 + (1+\phi_1)\mu}{(1+\phi_1)(\eta_1+\mu)R_1} + \frac{((1+\phi_1)-\phi_2)\eta_1\mu}{(1+\phi_1)\beta_1\Lambda},\\
\Leftrightarrow\ &\frac{1}{R_2} < \frac{\mu\phi_2\eta_1R_1 + (1+\phi_1)\mu^2 + ((1+\phi_1)-\phi_2)\eta_1\mu}{(1+\phi_1)\beta_1\Lambda},\\
\Leftrightarrow\ &R_2 > \frac{\beta_1\Lambda}{\mu\left(\mu + \eta_1 + \eta_1(R_1-1)\frac{\phi_2}{(1+\phi_1)}\right)}.
\end{aligned} \tag{3.7}$$

Therefore, by combining Conditions (3.4)–(3.7) above, it follows that $\bar{E}$ has biological significance if and only if $\widetilde{R}_1 < R_2 < R_1$.

For the endemic equilibrium $\hat{E}(\hat{s}, 0, \hat{i}_A, \hat{r}_1, \hat{i}_2)$, we have

$$\begin{aligned}
\hat{s} &= \frac{\eta_A + \mu}{\beta_A} = \frac{\Lambda}{\mu}\frac{1}{R_A},\\
\hat{r}_1 &= \frac{\eta_2 + \mu}{\phi_2\beta_2} - \frac{(1+\phi_1)(\eta_A+\mu)}{\phi_2\beta_A} = \frac{(1+\phi_1)}{\phi_2}\frac{\Lambda}{\mu}(\frac{1}{R_2} - \frac{1}{R_A}),\\
\hat{i}_A &= \frac{\mu(R_A - R_2)(((1+\phi_1)-\phi_2)\mu(\eta_A+\mu) + \phi_2\beta_A\Lambda)}{\phi_2\beta_A(\Lambda\beta_A - \mu^2 R_2)},\\
\hat{i}_2 &= \frac{\Lambda\beta_A\eta_A}{(\eta_A+\mu)(\beta_A(\eta_2+\mu) - (1+\phi_1)\beta_2\mu)} - \frac{\mu(\beta_A(\eta_2+\mu) - (1+\phi_1)\beta_2\mu - ((1+\phi_1)-\phi_2)\beta_2\eta_A)}{\phi_2\beta_2(\beta_A(\eta_2+\mu) - (1+\phi_1)\beta_2\mu)}.
\end{aligned}$$

Analogously, $\hat{E}$ is biologically meaningful if and only if $\widetilde{R}_A < R_2 < R_A$.

4. Stability analysis

4.1. Stability of the boundary equilibria

Theorem 4.1. *For System* (2.2)*, the following conclusions hold:*
(1) If E_1 exists (i.e., $R_1 > 1$) and satisfies $R_1 > R_A$, $R_1 > \widetilde{R}_1 > R_2$, then the boundary equilibrium E_1 of the system is locally asymptotically stable.
(2) If E_A exists (i.e., $R_A > 1$) and satisfies $R_A > R_1$, $R_A > \widetilde{R}_A > R_2$, then the boundary equilibrium E_A of the system is locally asymptotically stable.
(3) If E_2 exists (i.e., $R_2 > 1$) and satisfies $R_2 > R_1$, $R_2 > R_A$, then the boundary equilibrium E_2 of the system is locally asymptotically stable.

Proof. The local stability of an equilibrium point is determined by the eigenvalues of its corresponding Jacobian matrix evaluated at each equilibrium. First, we analyze the local stability of the boundary equilibrium E_1. The Jacobian matrix of System (2.2) at E_1 is given by

$$\begin{pmatrix}
-\beta_1\frac{\Lambda}{\eta_1+\mu} & -(\eta_1+\mu) & -\beta_A\frac{\eta_1+\mu}{\beta_1} & 0 & -(1+\phi_1)\beta_2\frac{\eta_1+\mu}{\beta_1}\\
\beta_1\frac{\Lambda}{\eta_1+\mu} - \mu & 0 & 0 & 0 & 0\\
0 & 0 & \beta_A\frac{\eta_1+\mu}{\beta_1} - (\eta_A+\mu) & 0 & 0\\
0 & \eta_1 & \eta_A & -\mu & -\phi_2\beta_2\left(\frac{\eta_1\Lambda}{\mu(\eta_1+\mu)} - \frac{\eta_1}{\beta_1}\right)\\
0 & 0 & 0 & 0 & (1+\phi_1)\beta_2\dfrac{\eta_1+\mu}{\beta_1} + \phi_2\beta_2\left(\dfrac{\eta_1\Lambda}{\mu(\eta_1+\mu)} - \dfrac{\eta_1}{\beta_1}\right) - (\eta_2+\mu)
\end{pmatrix}.$$

The Jacobian matrix yields the characteristic equation

$$\begin{aligned}
&-(\lambda+\mu)(\lambda^2 + \beta_1(\frac{\Lambda}{\eta_1+\mu})\lambda + \eta_1\beta_1(\frac{\Lambda}{\eta_1+\mu}) + \mu\beta_1(\frac{\Lambda}{\eta_1+\mu}) - \mu\eta_1 - \mu^2)(-\lambda + \beta_A(\frac{\eta_1+\mu}{\beta_1})\\
&-\mu-\eta_A)(-\lambda + \beta_2\phi_2(\frac{\Lambda\eta_1}{\mu(\eta_1+\mu)} - \frac{\eta_1}{\beta_1}) + \beta_2(1+\phi_1)(\frac{\eta_1+\mu}{\beta_1}) - \mu - \eta_2) = 0.
\end{aligned}$$

Clearly, three eigenvalues are obtained directly as follows:

$$\lambda_1 = -\mu, \quad \lambda_2 = \beta_A(\frac{\eta_1+\mu}{\beta_1}) - (\eta_A+\mu) = \frac{\Lambda}{\mu}\beta_A(\frac{1}{R_1} - \frac{1}{R_A}),$$
$$\lambda_3 = \beta_2\phi_2(\frac{\Lambda\eta_1}{\mu(\eta_1+\mu)} - \frac{\eta_1}{\beta_1}) + \beta_2(1+\phi_1)(\frac{\eta_1+\mu}{\beta_1}) - (\eta_2+\mu).$$

The remaining two eigenvalues (λ_4, λ_5) are determined by the characteristic equation

$$\lambda^2 + W_1\lambda + W_2 = 0,$$

where

$$W_1 = \beta_1(\frac{\Lambda}{\eta_1+\mu}), \quad W_2 = \eta_1\beta_1(\frac{\Lambda}{\eta_1+\mu}) + \mu\beta_1(\frac{\Lambda}{\eta_1+\mu}) - \mu\eta_1 - \mu^2.$$

Thus, according to Vieta's theorem, it follows that

$$\begin{cases} \lambda_4 + \lambda_5 = -\beta_1(\frac{\Lambda}{\eta_1+\mu}), \\ \lambda_4 \cdot \lambda_5 = \beta_1(\frac{\Lambda}{\eta_1+\mu})(\eta_1+\mu) - \mu(\eta_1+\mu) = \mu(\eta_1+\mu)(R_1-1). \end{cases} \tag{4.1}$$

Evidently, $-\beta_1(\frac{\Lambda}{\eta_1+\mu}) < 0$ holds, i.e., $\lambda_4 + \lambda_5 < 0$. In this case, Eq (4.1) determines whether the eigenvalues λ_4 and λ_5 have negative real parts. If $R_1 > 1$, then $\lambda_4 \cdot \lambda_5 > 0$. Combined with Eq (4.1), this implies that both eigenvalues satisfy $\lambda_4 < 0$ and $\lambda_5 < 0$.

Furthermore, to ensure $\lambda_2 < 0$, the following condition must hold: $\frac{\Lambda}{\mu}\beta_A(\frac{1}{R_1} - \frac{1}{R_A}) < 0$, i.e., $R_1 > R_A$. Similarly, achieving $\lambda_3 < 0$ is equivalent to

$$\begin{aligned}
& \beta_2\phi_2(\frac{\Lambda\eta_1}{\mu(\eta_1+\mu)} - \frac{\eta_1}{\beta_1}) + \beta_2(1+\phi_1)(\frac{\eta_1+\mu}{\beta_1}) - (\eta_2+\mu) < 0, \\
\Leftrightarrow \quad & \frac{\phi_2}{(1+\phi_1)}(\frac{\Lambda\eta_1}{\mu(\eta_1+\mu)} - \frac{\eta_1}{\beta_1}) + \frac{\eta_1+\mu}{\beta_1} < \frac{\eta_2+\mu}{(1+\phi_1)\beta_2}, \\
\Leftrightarrow \quad & \frac{\phi_2}{(1+\phi_1)}\frac{\eta_1}{\beta_1}(R_1-1) + \frac{\eta_1+\mu}{\beta_1} < \frac{\Lambda}{\mu}\frac{1}{R_2}, \\
\Leftrightarrow \quad & \frac{\mu\left(\mu+\eta_1+\eta_1(R_1-1)\frac{\phi_2}{(1+\phi_1)}\right)}{\Lambda\beta_1} < \frac{1}{R_2}, \\
\Leftrightarrow \quad & R_2 < \frac{\beta_1\Lambda}{\mu\left(\mu+\eta_1+\eta_1(R_1-1)\frac{\phi_2}{(1+\phi_1)}\right)}.
\end{aligned}$$

To sum up, when satisfying all

$$R_1 > 1, \ R_1 > R_A, \ \widetilde{R}_1 > R_2,$$

the boundary equilibrium E_1 is locally asymptotically stable. It can be observed that $R_1 > \widetilde{R}_1$; therefore, E_1 is locally asymptotically stable if $R_1 > 1$, $R_1 > R_A$, and $R_1 > \widetilde{R}_1 > R_2$ hold. Conversely, if $R_1 < R_A$ or $R_1 < R_2$, then the boundary equilibrium E_1 is unstable.

Similarly, for the boundary equilibrium E_A, the Jacobian matrix of System (2.2) at E_A is given by

$$\begin{pmatrix} -\beta_A\frac{\Lambda}{\eta_A+\mu} & -\beta_1\frac{\eta_A+\mu}{\beta_A} & -(\eta_A+\mu) & 0 & -(1+\phi_1)\beta_2\frac{\eta_A+\mu}{\beta_A} \\ 0 & \beta_1\frac{\eta_A+\mu}{\beta_A}-(\eta_1+\mu) & 0 & 0 & 0 \\ \beta_A\frac{\Lambda}{\eta_A+\mu}-\mu & 0 & 0 & 0 & 0 \\ 0 & \eta_1 & \eta_A & -\mu & -\phi_2\beta_2\left(\frac{\eta_A\Lambda}{\mu(\eta_A+\mu)}-\frac{\eta_A}{\beta_A}\right) \\ 0 & 0 & 0 & 0 & (1+\phi_1)\beta_2\frac{\eta_A+\mu}{\beta_A}+\phi_2\beta_2\left(\frac{\eta_A\Lambda}{\mu(\eta_A+\mu)}-\frac{\eta_A}{\beta_A}\right)-(\eta_2+\mu) \end{pmatrix}.$$

Based on calculations, when all the following conditions are satisfied:

$$R_A > 1,\ R_A > R_1,\ \widetilde{R}_A > R_2,$$

the boundary equilibrium E_A is locally asymptotically stable. Likewise, since $R_A > \widetilde{R}_A$, when $R_A > 1$, $R_A > R_1$, and $R_A > \widetilde{R}_A > R_2$ are satisfied, E_A is locally asymptotically stable. Conversely, if $R_A < R_1$ or $R_A < R_2$, then the boundary equilibrium E_A becomes unstable.

Finally, for the boundary equilibrium E_2 of System (2.2), the Jacobian matrix evaluated at E_2 is

$$\begin{pmatrix} -\beta_2(1+\phi_1)\frac{\Lambda}{\eta_2+\mu} & -\beta_1\frac{\eta_2+\mu}{\beta_2(1+\phi_1)} & -\beta_A\frac{\eta_2+\mu}{\beta_2(1+\phi_1)} & 0 & -(\eta_2+\mu) \\ 0 & \beta_1\frac{\eta_2+\mu}{\beta_2(1+\phi_1)}-(\eta_1+\mu) & 0 & 0 & 0 \\ 0 & 0 & \beta_A\frac{\eta_2+\mu}{\beta_2(1+\phi_1)}-(\eta_A+\mu) & 0 & 0 \\ 0 & \eta_1 & \eta_A & -\beta_2\phi_2\left(\frac{\Lambda}{\eta_2+\mu}-\frac{\mu}{\beta_2(1+\phi_1)}\right)-\mu & 0 \\ \beta_2(1+\phi_1)\frac{\Lambda}{\eta_2+\mu}-\mu & 0 & 0 & \beta_2\phi_2\left(\frac{\Lambda}{\eta_2+\mu}-\frac{\mu}{\beta_2(1+\phi_1)}\right) & 0 \end{pmatrix}.$$

The Jacobian matrix yields the following three immediate eigenvalues:

$$\begin{aligned} \lambda_1 &= -\beta_2\phi_2\left(\frac{\Lambda}{\eta_2+\mu}-\frac{\mu}{\beta_2(1+\phi_1)}\right)-\mu = -\frac{\phi_2\mu}{(1+\phi_1)}(R_2-1)-\mu, \\ \lambda_2 &= \beta_1\left(\frac{\eta_2+\mu}{\beta_2(1+\phi_1)}\right)-(\eta_1+\mu) = \frac{\Lambda\beta_1}{\mu}\left(\frac{1}{R_2}-\frac{1}{R_1}\right), \\ \lambda_3 &= \beta_A\left(\frac{\eta_2+\mu}{\beta_2(1+\phi_1)}\right)-(\eta_A+\mu) = \frac{\Lambda\beta_A}{\mu}\left(\frac{1}{R_2}-\frac{1}{R_A}\right). \end{aligned}$$

The remaining two eigenvalues λ_4 and λ_5 are determined by the characteristic equation

$$H_1\lambda^2 + H_2\lambda + H_3 = 0,$$

where

$$\begin{aligned} &H_1 = -(\eta_2+\mu), \quad H_2 = -\beta_2(1+\phi_1)\Lambda, \\ &H_3 = -\beta_2\eta_2(1+\phi_1)\Lambda - \beta_2\mu(1+\phi_1)\Lambda + \mu^3 + \mu\eta_2^2 + 2\mu^2\eta_2 = -\beta_2(1+\phi_1)\Lambda(\eta_2+\mu) + \mu(\mu+\eta_2)^2. \end{aligned}$$

It follows from Vieta's theorem that

$$\begin{cases} \lambda_4 + \lambda_5 = -\dfrac{\beta_2(1+\phi_1)\Lambda}{\eta_2+\mu}, \\ \lambda_4 \cdot \lambda_5 = \dfrac{-\beta_2(1+\phi_1)\Lambda(\eta_2+\mu)+\mu(\mu+\eta_2)^2}{-(\eta_2+\mu)} = \beta_2(1+\phi_1)\Lambda - \mu(\mu+\eta_2). \end{cases}$$

If the following conditions hold:

$$R_2 > 1,\ R_2 > R_1,\ R_2 > R_A,$$

then $\lambda_2 < 0$, $\lambda_3 < 0$, $\lambda_4 < 0$, $\lambda_5 < 0$. In this case, all five eigenvalues of the Jacobian matrix have negative real parts, and the boundary equilibrium E_2 is locally asymptotically stable in System (2.2). That is, when $R_2 > 1$, $R_2 > R_1$, and $R_2 > R_A$ are satisfied, E_2 is locally asymptotically stable; conversely, E_2 is unstable if $R_2 < R_1$ or $R_2 < R_A$.

Next, we examine the global asymptotic stability of the boundary equilibria. To establish this, we construct classical Lyapunov functions leveraging the properties of the function

$$f(x) = x - 1 - \ln(x).$$

Theorem 4.2. *Suppose that the boundary equilibrium E_1 exists (i.e., $R_1 > 1$) and satisfies*

$$R_1 > \widetilde{\widetilde{R}}_A > R_A,\ R_1 > \widetilde{R}_1 > R_2,$$

then E_1 is globally asymptotically stable. Conversely, if

$$R_1 < R_A \text{ or } R_1 < R_2$$

holds, E_1 exists but is unstable.

Proof. Begin by considering the following Lyapunov function:

$$V(s, i_1, i_A, r_1, i_2) = s_1(\frac{s}{s_1} - 1 - \ln\frac{s}{s_1}) + i_{11}(\frac{i_1}{i_{11}} - 1 - \ln\frac{i_1}{i_{11}}) + i_A + r_{11}(\frac{r_1}{r_{11}} - 1 - \ln\frac{r_1}{r_{11}}) + i_2.$$

Clearly, the function V is non-negative in R^5_+ and equals zero at $E_1(s_1, i_{11}, 0, r_{11}, 0)$. To establish stability, we prove that V' is negative definite. Differentiating V along the trajectories of System (2.2) yields

$$\begin{aligned}
\frac{dV}{dt} &= (1-\frac{s_1}{s})\frac{ds}{dt} + (1-\frac{i_{11}}{i_1})\frac{di_1}{dt} + \frac{di_A}{dt} + (1-\frac{r_{11}}{r_1})\frac{dr_1}{dt} + \frac{di_2}{dt}, \\
(1-\frac{s_1}{s})\frac{ds}{dt} &= (1-\frac{s_1}{s})(\Lambda - \beta_1 s i_1 - \beta_A s i_A - (1+\phi_1)\beta_2 s i_2 - \mu s) \\
&= \Lambda - \beta_1 s i_1 - \beta_A s i_A - (1+\phi_1)\beta_2 s i_2 - \mu s - \frac{s_1}{s}\Lambda + \beta_1 s_1 i_1 + \beta_A s_1 i_A + (1+\phi_1)\beta_2 s_1 i_2 + \mu s_1, \\
(1-\frac{i_{11}}{i_1})\frac{di_1}{dt} &= (1-\frac{i_{11}}{i_1})(\beta_1 s i_1 - \eta_1 i_1 - \mu i_1) = \beta_1 s i_1 - \eta_1 i_1 - \mu i_1 - \beta_1 s i_{11} + \eta_1 i_{11} + \mu i_{11}, \\
\frac{di_A}{dt} &= \beta_A s i_A - \eta_A i_A - \mu i_A, \\
(1-\frac{r_{11}}{r_1})\frac{dr_1}{dt} &= (1-\frac{r_{11}}{r_1})(\eta_1 i_1 + \eta_A i_A - \phi_2\beta_2 r_1 i_2 - \mu r_1) \\
&= \eta_1 i_1 + \eta_A i_A - \phi_2\beta_2 r_1 i_2 - \mu r_1 - \frac{r_{11}}{r_1}\eta_1 i_1 - \frac{r_{11}}{r_1}\eta_A i_A + \phi_2\beta_2 r_{11} i_2 + \mu r_{11},
\end{aligned}$$

$$\frac{di_2}{dt} = (1+\phi_1)\beta_2 s i_2 + \phi_2\beta_2 r_1 i_2 - \eta_2 i_2 - \mu i_2.$$

From the formulation above, we derive

$$\begin{aligned}
\frac{dV}{dt} &= \Lambda - \mu s - \frac{s_1}{s}\Lambda + \beta_1 s_1 i_1 + \beta_A s_1 i_A + (1+\phi_1)\beta_2 s_1 i_2 + \mu s_1 - \mu i_1 - \beta_1 s i_{11} + \eta_1 i_{11} + \mu i_{11} \\
&\quad - \mu i_A - \mu r_1 - \frac{r_{11}}{r_1}\eta_1 i_1 - \frac{r_{11}}{r_1}\eta_A i_A + \phi_2\beta_2 r_{11} i_2 + \mu r_{11} - \eta_2 i_2 - \mu i_2 \\
&= \mu s_1 R_1 - \mu s - \frac{s_1}{s}\mu s_1 R_1 + (\eta_1+\mu) i_1 + \beta_A s_1 i_A + (1+\phi_1)\beta_2 s_1 i_2 + \mu s_1 - \mu i_1 - \mu s(R_1 - 1) \\
&\quad + \mu s_1(R_1 - 1) - \mu i_A - \mu r_1 - \frac{r_{11}}{r_1}\mu r_{11} - \frac{r_{11}}{r_1}\eta_A i_A + \phi_2\beta_2 r_{11} i_2 + \mu r_{11} - \eta_2 i_2 - \mu i_2 \\
&= 2\mu s_1 R_1 - \frac{s_1}{s}\mu s_1 R_1 - \mu s R_1 + 2\mu r_{11} - \frac{r_{11}}{r_1}\mu r_{11} - \mu r_1 + (\beta_A s_1 - \mu) i_A \\
&\quad + ((1+\phi_1)\beta_2 s_1 + \phi_2\beta_2 r_{11} - (\eta_2+\mu)) i_2 - \frac{r_{11}}{r_1}\eta_A i_A \\
&= \mu s_1 R_1 (2 - \frac{s_1}{s} - \frac{s}{s_1}) + \mu r_{11}(2 - \frac{r_{11}}{r_1} - \frac{r_1}{r_{11}}) + (\beta_A s_1 - \mu) i_A + ((1+\phi_1)\beta_2 s_1 + \phi_2\beta_2 r_{11} \\
&\quad - (\eta_2+\mu)) i_2 - \frac{r_{11}}{r_1}\eta_A i_A.
\end{aligned}$$

Under the assumptions that $R_1 > \widetilde{\widetilde{R}}_A$ and $\widetilde{R}_1 > R_2$, it follows that $\frac{dV}{dt}|_{(3.1)} \le 0$, and E_1 is locally stable. It can be observed that E_1 is the largest positively invariant set contained in $\frac{dV}{dt}|_{(3.1)} = 0$. Therefore, by LaSalle's invariance principle [20], the boundary equilibrium E_1 is globally asymptotically stable for System (2.2).

Theorem 4.3. *Suppose the boundary equilibrium E_A exists (i.e., $R_A > 1$) and satisfies*

$$R_A > \widetilde{\widetilde{R}}_1 > R_1,\ R_A > \widetilde{R}_A > R_2.$$

Then E_A is globally asymptotically stable. Conversely, if

$$R_A < R_1 \text{ or } R_A < R_2$$

holds, E_A exists but is unstable.

Proof. Consider the Lyapunov function

$$V(s, i_1, i_A, r_1, i_2) = s_A(\frac{s}{s_A} - 1 - \ln\frac{s}{s_A}) + i_1 + i_{AA}(\frac{i_A}{i_{AA}} - 1 - \ln\frac{i_A}{i_{AA}}) + r_{1A}(\frac{r_1}{r_{1A}} - 1 - \ln\frac{r_1}{r_{1A}}) + i_2.$$

The function V is positive definite in R^5_+ and reaches zero at $E_A(s_A, 0, i_{AA}, r_{1A}, 0)$. We need to show that V' is negative definite. Computing the derivative along the trajectories of System (2.2) yields

$$\frac{dV}{dt} = (1 - \frac{s_A}{s})\frac{ds}{dt} + \frac{di_1}{dt} + (1 - \frac{i_{AA}}{i_A})\frac{di_A}{dt} + (1 - \frac{r_{1A}}{r_1})\frac{dr_1}{dt} + \frac{di_2}{dt}.$$

We then obtain

$$\begin{aligned}\frac{dV}{dt} &= \Lambda - \mu s - \frac{s_A}{s}\Lambda + \beta_1 s_A i_1 + \beta_A s_A i_A + (1+\phi_1)\beta_2 s_A i_2 + \mu s_A - \mu i_1 - \mu i_A - \beta_A s i_{AA} \\ &\quad + \eta_A i_{AA} + \mu i_{AA} - \mu r_1 - \frac{r_{1A}}{r_1}\eta_1 i_1 - \frac{r_{1A}}{r_1}\eta_A i_A + \phi_2\beta_2 r_{1A} i_2 + \mu r_{1A} - \eta_2 i_2 - \mu i_2 \\ &= 2\mu s_A R_A - \frac{s_A}{s}\mu s_A R_A - \mu s R_A + 2\mu r_{1A} - \frac{r_{1A}}{r_1}\mu r_{1A} - \mu r_1 + (\beta_1 s_A - \mu) i_A \\ &\quad + ((1+\phi_1)\beta_2 s_A + \phi_2\beta_2 r_{1A} - (\eta_2 + \mu)) i_2 - \frac{r_{1A}}{r_1}\eta_1 i_1 \\ &= \mu s_A R_A (2 - \frac{s_A}{s} - \frac{s}{s_A}) + \mu r_{1A}(2 - \frac{r_{1A}}{r_1} - \frac{r_1}{r_{1A}}) + (\beta_1 s_A - \mu) i_A + ((1+\phi_1)\beta_2 s_A + \phi_2\beta_2 r_{1A} \\ &\quad - (\eta_2 + \mu)) i_2 - \frac{r_{1A}}{r_1}\eta_1 i_1.\end{aligned}$$

Under the hypothesis that $R_A > \widetilde{\widetilde{R}}_1$ and $\widetilde{R}_A > R_2$, it follows that $\frac{dV}{dt}|_{(3.1)} \leq 0$, and thus the boundary equilibrium E_A is locally stable. Furthermore, E_A constitutes the maximal positively invariant set contained in $\frac{dV}{dt}|_{(3.1)} = 0$. Consequently, by LaSalle's invariance principle [20], E_A is globally asymptotically stable for System (2.2).

Theorem 4.4. *If we suppose that the boundary equilibrium E_2 exists (i.e., $R_2 > 1$) and satisfies*

$$R_2 > \widetilde{\widetilde{R}}_1 > R_1,\ R_2 > \widetilde{\widetilde{R}}_A > R_A,$$

then E_2 is globally asymptotically stable. Conversely, if

$$R_2 < R_1 \text{ or } R_2 < R_A$$

holds, E_2 exists but is unstable.

Proof. Consider

$$V(s, i_1, i_A, r_1, i_2) = s_2(\frac{s}{s_2} - 1 - \ln\frac{s}{s_2}) + i_1 + i_A + r_1 + i_{22}(\frac{i_2}{i_{22}} - 1 - \ln\frac{i_2}{i_{22}}).$$

The function V is positive definite in R^5_+ and reaches zero at $E_2(s_2, 0, 0, 0, i_{22})$. We need to show that V' is negative definite. Differentiating V along the trajectories of System (2.2) yields

$$\begin{aligned}\frac{dV}{dt} &= (1 - \frac{s_1}{s})\frac{ds}{dt} + \frac{di_1}{dt} + \frac{di_A}{dt} + \frac{dr_1}{dt} + (1 - \frac{i_{22}}{i_2})\frac{di_2}{dt} \\ &= \Lambda - \mu s - \frac{s_2}{s}\Lambda + \beta_1 s_2 i_1 + \beta_A s_2 i_A + (1+\phi_1)\beta_2 s_2 i_2 + \mu s_2 - \mu i_1 - \mu i_A - \mu r_1 - \eta_2 i_2 \\ &\quad - \mu i_2 - (1+\phi_1)\beta_2 s i_{22} - \phi_2\beta_2 r_1 i_{22} + \eta_2 i_{22} + \mu i_{22} \\ &= \mu s_2 R_2 (2 - \frac{s_2}{s} - \frac{s}{s_2}) + (\beta_1 s_2 - \mu) i_1 + (\beta_A s_2 - \mu) i_A - \phi_2\beta_2 r_1 i_{22} - \mu r_1.\end{aligned}$$

If $R_2 > \frac{\eta_1 + \mu}{\mu}R_1$, $R_2 > \frac{\eta_A + \mu}{\mu}R_A$, then $\frac{dV}{dt}|_{(3.1)} \leq 0$, and E_2 is locally stable. Moreover, E_2 constitutes the largest positively invariant set contained in $\frac{dV}{dt}|_{(3.1)} = 0$. Therefore, by LaSalle's invariance principle [20], the boundary equilibrium E_2 is globally asymptotically stable for System (2.2).

4.2. Stability of endemic equilibria

Theorem 4.5. *For System* (2.2)*, the following conclusions hold:*
1) If $\bar{E}$ exists (i.e., $\widetilde{R}_1 < R_2 < R_1$) and satisfies $R_1 > R_A$, then the endemic equilibrium $\bar{E}$ of the system is locally asymptotically stable.
2) If $\hat{E}$ exists (i.e., $\widetilde{R}_A < R_2 < R_A$) and satisfies $R_A > R_1$, then the endemic equilibrium $\hat{E}$ of the system is locally asymptotically stable.

Proof. For the endemic equilibrium $\bar{E}(\bar{s}, \bar{i}_1, 0, \bar{r}_1, \bar{i}_2)$, the Jacobian matrix of System (2.2) at $\bar{E}$ is given by

$$\begin{pmatrix} -\beta_1\bar{i}_1 - (1+\phi_1)\beta_2\bar{i}_2 - \mu & -\beta_1\bar{s} & -\beta_A\bar{s} & 0 & -(1+\phi_1)\beta_2\bar{s} \\ \beta_1\bar{i}_1 & 0 & 0 & 0 & 0 \\ 0 & 0 & \beta_A\bar{s} - (\eta_A+\mu) & 0 & 0 \\ 0 & \eta_1 & \eta_A & -\phi_2\beta_2\bar{i}_2 - \mu & -\phi_2\beta_2\bar{r}_1 \\ (1+\phi_1)\beta_2\bar{i}_2 & 0 & 0 & \phi_2\beta_2\bar{i}_2 & 0 \end{pmatrix}.$$

The Jacobian matrix yields one immediate eigenvalue

$$\lambda_1 = \beta_A\bar{s} - (\eta_A + \mu) = \frac{\beta_A\Lambda}{\mu}\left(\frac{1}{R_1} - \frac{1}{R_A}\right). \tag{4.2}$$

The remaining four eigenvalues are determined by the following characteristic equation:

$$\lambda^4 + M_1\lambda^3 + M_2\lambda^2 + M_3\lambda + M_4 = 0,$$

where

$$\begin{aligned} M_1 &= m_1 + (1+\phi_1+\phi_2)m_2 + 2\mu, \\ M_2 &= (m_1 + (1+\phi_1)m_2 + \mu)(\phi_2 m_2 + \mu) + m_1 m_3 + m_2(\phi_2^2 m_4 + (1+\phi_1)^2 m_5), \\ M_3 &= (m_1 + (1+\phi_1)m_2 + \mu)\phi_2^2 m_2 m_4 + (\phi_2 m_2 + \mu)(m_1 m_3 + (1+\phi_1)^2 m_2 m_5), \\ M_4 &= \phi_2 m_1 m_2(\phi_2 m_3 m_4 + (1+\phi_1)\eta_1 m_5). \\ m_1 &= \beta_1\bar{i}_1,\ m_2 = \beta_2\bar{i}_2,\ m_3 = \beta_1\bar{s},\ m_4 = \beta_2\bar{r}_1,\ m_5 = \beta_2\bar{s}. \end{aligned}$$

Equation (4.2) shows that one of the eigenvalues is $\lambda_1 = \frac{\beta_A\Lambda}{\mu}\left(\frac{1}{R_1} - \frac{1}{R_A}\right)$, and if $R_1 > R_A$, then $\lambda_1 < 0$.

To ensure that all roots of the quartic equation have negative real parts, we apply the Hurwitz criterion. From the existence conditions of $\bar{E}(\bar{s}, \bar{i}_1, 0, \bar{r}_1, \bar{i}_2)$, we know that $\bar{E}$ exists if and only if $\widetilde{R}_1 < R_2 < R_1$ holds. Under this condition, all coefficients (M_1, M_2, M_3, M_4) are positive, and the leading principal minors are positive.

Therefore, by the Hurwitz criterion, System (2.2) is locally asymptotically stable at the endemic equilibrium $\bar{E}$. Conversely, if $R_1 < R_A$, then the endemic equilibrium $\bar{E}$ exists but is unstable.

Analogously, for the endemic equilibrium $\hat{E}(\hat{s}, 0, \hat{i}_A, \hat{r}_1, \hat{i}_2)$, the Jacobian matrix of System (2.2)

evaluated at $\hat{E}$ is given by

$$\begin{pmatrix} -\beta_A\hat{i}_A - (1+\phi_1)\beta_2\hat{i}_2 - \mu & -\beta_1\hat{s} & -\beta_A\hat{s} & 0 & -(1+\phi_1)\beta_2\hat{s} \\ 0 & \beta_1\hat{s} - (\eta_1+\mu) & 0 & 0 & 0 \\ \beta_A\hat{i}_A & 0 & 0 & 0 & 0 \\ 0 & \eta_1 & \eta_A & -\phi_2\beta_2\hat{i}_2 - \mu & -\phi_2\beta_2\hat{r}_1 \\ (1+\phi_1)\beta_2\hat{i}_2 & 0 & 0 & \phi_2\beta_2\hat{i}_2 & 0 \end{pmatrix}.$$

Through computation, if

$$R_A > R_1,$$

then the endemic equilibrium $\hat{E}$ is locally asymptotically stable. Conversely, if $R_A < R_1$, then $\hat{E}$ exists but is unstable.

Next, we use the geometric approach proposed in [21,22] to analyze the global asymptotic stability of the endemic equilibria $\bar{E}$ and $\hat{E}$. This approach is commonly applied to three-dimensional systems; we extend its application to the five-dimensional system below.

For System (2.2), we have

$$\widetilde{\Omega} = \left\{ (s(t), i_1(t), i_A(t), r_1(t), i_2(t)) \;\middle|\; 0 \le s(t) + i_1(t) + i_A(t) + r_1(t) + i_2(t) \le \frac{\Lambda}{\mu} \right\}$$

forms a positively invariant set. According to Theorem 3.2, when $\widetilde{R}_1 < R_2 < R_1$, there is a unique endemic equilibrium $\bar{E}$ in the interior of $\widetilde{\Omega}$; when $\widetilde{R}_A < R_2 < R_A$, there is a unique endemic equilibrium $\hat{E}$ in the interior of $\widetilde{\Omega}$.

Theorem 4.6. *If the endemic equilibrium $\bar{E}$ exists and the system satisfies the condition*

$$\begin{aligned} \mu > \max\Big\{ & 2(\bar{b}+\eta_1) + \frac{(\beta_A + (1+\phi_1)\beta_2)\Lambda}{\mu}, \bar{b} + \frac{(2\beta_1 + 2\beta_A)\Lambda}{\mu}, \\ & \bar{b} + \eta_A + \frac{(2\beta_1 + (1+\phi_1)\beta_2)\Lambda}{\mu}, 2\bar{b} + \eta_2 + \frac{\beta_A\Lambda}{\mu}, \eta_1 + \eta_A \Big\}, \end{aligned} \tag{4.3}$$

then System (2.2) *is globally asymptotically stable at $\bar{E}(\bar{s}, \bar{i}_1, 0, \bar{r}_1, \bar{i}_2)$.*

Proof. Initially, the region $\widetilde{\Omega}$ is simply connected in R^5_+, and when $\widetilde{R}_1 < R_2 < R_1$, there is a unique endemic equilibrium $\bar{E}$ in the interior of $\widetilde{\Omega}$. Furthermore, by Theorem 3.1, the instability of the disease-free equilibrium implies the uniform persistence of System (2.2) (see [23]). Specifically, a constant $n > 0$ exists such that any solution $x(t, x_0) = (s(t), i_1(t), i_A(t), r_1(t), i_2(t))$ with $x_0 = (s(0), i_1(0), i_A(0), r_1(0), i_2(0))$ in the interior of $\widetilde{\Omega}$ satisfies

$$\min\left\{ \liminf_{t\to\infty} s(t), \liminf_{t\to\infty} i_1(t), \liminf_{t\to\infty} i_A(t), \liminf_{t\to\infty} r_1(t), \liminf_{t\to\infty} i_2(t) \right\} > n.$$

The uniform persistence and boundedness of $\widetilde{\Omega}$ are equivalent to the existence of a compact absorbing set K in the interior of $\widetilde{\Omega}$ (see [24]). Therefore, to prove global stability, it suffices to verify the condition $\overline{q} < 0$, where

$$\overline{q} = \limsup_{t\to\infty} \sup_{x_0\in\Gamma} \frac{1}{t} \int_0^t \sigma(Q(x(s, x_0)))\, ds.$$

The Jacobian matrix J of System (2.2) is

$$\begin{pmatrix} -\beta_1 i_1 - \beta_A i_A - (1+\phi_1)\beta_2 i_2 - \mu & -\beta_1 s & -\beta_A s & 0 & -(1+\phi_1)\beta_2 s \\ \beta_1 i_1 & \beta_1 s - (\eta_1 + \mu) & 0 & 0 & 0 \\ \beta_A i_A & 0 & \beta_A s - (\eta_A + \mu) & 0 & 0 \\ 0 & \eta_1 & \eta_A & -\phi_2\beta_2 i_2 - \mu & -\phi_2\beta_2 r_1 \\ (1+\phi_1)\beta_2 i_2 & 0 & 0 & \phi_2\beta_2 i_2 & (1+\phi_1)\beta_2 s + \phi_2\beta_2 r_1 - (\eta_2 + \mu) \end{pmatrix}.$$

For a 5×5 matrix J, its second additive compound $J^{[2]}$ is defined as

$$\begin{pmatrix} M_1 & 0 & 0 & 0 & \beta_A s & 0 & (1+\phi_1)\beta_2 s & 0 & 0 & 0 \\ 0 & M_2 & 0 & 0 & -\beta_1 s & 0 & 0 & 0 & (1+\phi_1)\beta_2 s & 0 \\ \eta_1 & \eta_A & M_3 & -\phi_2\beta_2 r_1 & 0 & -\beta_1 s & 0 & -\beta_A s & 0 & (1+\phi_1)\beta_2 s \\ 0 & 0 & \phi_2\beta_2 i_2 & M_4 & 0 & 0 & -\beta_1 s & 0 & -\beta_A s & 0 \\ -\beta_A i_A & \beta_1 i_1 & 0 & 0 & M_5 & 0 & 0 & 0 & 0 & 0 \\ 0 & 0 & \beta_1 i_1 & 0 & \eta_A & M_6 & -\phi_2\beta_2 r_1 & 0 & 0 & 0 \\ -(1+\phi_1)\beta_2 i_2 & 0 & 0 & \beta_1 i_1 & 0 & \phi_2\beta_2 i_2 & M_7 & 0 & 0 & 0 \\ 0 & 0 & \beta_A i_A & 0 & -\eta_1 & 0 & 0 & M_8 & -\phi_2\beta_2 r_1 & 0 \\ 0 & -(1+\phi_1)\beta_2 i_2 & 0 & \beta_A i_A & 0 & 0 & 0 & \phi_2\beta_2 i_2 & M_9 & 0 \\ 0 & 0 & -(1+\phi_1)\beta_2 i_2 & 0 & 0 & 0 & \eta_1 & 0 & \eta_A & M_{10} \end{pmatrix},$$

where

$$\begin{aligned} M_1 &= -\beta_1 i_1 - \beta_A i_A - (1+\phi_1)\beta_2 i_2 + \beta_1 s - \eta_1 - 2\mu, \\ M_2 &= -\beta_1 i_1 - \beta_A i_A - (1+\phi_1)\beta_2 i_2 + \beta_A s - \eta_A - 2\mu, \\ M_3 &= -\beta_1 i_1 - \beta_A i_A - (1+\phi_1)\beta_2 i_2 - \phi_2\beta_2 i_2 - 2\mu, \\ M_4 &= -\beta_1 i_1 - \beta_A i_A - (1+\phi_1)\beta_2 i_2 + (1+\phi_1)\beta_2 s + \phi_2\beta_2 r_1 - \eta_2 - 2\mu, \\ M_5 &= \beta_1 s + \beta_A s - \eta_1 - \eta_A - 2\mu, \quad M_6 = \beta_1 s - \phi_2\beta_2 i_2 - \eta_1 - 2\mu, \\ M_7 &= \beta_1 s + (1+\phi_1)\beta_2 s + \phi_2\beta_2 r_1 - \eta_1 - \eta_2 - 2\mu, \quad M_8 = \beta_A s - \phi_2\beta_2 i_2 - \eta_A - 2\mu, \\ M_9 &= \beta_A s + (1+\phi_1)\beta_2 s + \phi_2\beta_2 r_1 - \eta_A - \eta_2 - 2\mu, \\ M_{10} &= -\phi_2\beta_2 i_2 + (1+\phi_1)\beta_2 s + \phi_2\beta_2 r_1 - \eta_2 - 2\mu. \end{aligned}$$

Let

$$P = P(s, i_1, i_A, r_1, i_2) = diag(\frac{a_1}{i_1}, \frac{a_1}{i_1}, \frac{a_1}{i_1}, \frac{a_2}{i_A}, \frac{a_2}{i_A}, \frac{a_2}{i_A}, \frac{a_2}{i_A}, \frac{a_3}{i_2}, \frac{a_3}{i_2}, \frac{a_3}{i_2}),$$

where a_1, a_2, a_3 are three undetermined positive constants. We then have

$$P_f P^{-1} = diag(-\frac{i_1'}{i_1}, -\frac{i_1'}{i_1}, -\frac{i_1'}{i_1}, -\frac{i_A'}{i_A}, -\frac{i_A'}{i_A}, -\frac{i_A'}{i_A}, -\frac{i_A'}{i_A}, -\frac{i_2'}{i_2}, -\frac{i_2'}{i_2}, -\frac{i_2'}{i_2}).$$

Furthermore, for the matrix $Q(s, i_1, i_A, r_1, i_2) = P_f P^{-1} + PJ^{[2]}P^{-1}$, after partitioning it into blocks, it can be written in the following form:

$$Q(s, i_1, i_A, r_1, i_2) = \begin{pmatrix} Q_{11} & Q_{12} & Q_{13} & Q_{14} & Q_{15} & Q_{16} \\ Q_{21} & Q_{22} & Q_{23} & Q_{24} & Q_{25} & Q_{26} \\ Q_{31} & Q_{32} & Q_{33} & Q_{34} & Q_{35} & Q_{36} \\ Q_{41} & Q_{42} & Q_{43} & Q_{44} & Q_{45} & Q_{46} \\ Q_{51} & Q_{52} & Q_{53} & Q_{54} & Q_{55} & Q_{56} \\ Q_{61} & Q_{62} & Q_{63} & Q_{64} & Q_{65} & Q_{66} \end{pmatrix},$$

where Appendix A contains all entries Q_{ij} of Q.

Let $z = (z_1, z_2, z_3, z_4, z_5, z_6, z_7, z_8, z_9, z_{10})$ denote a vector in R^{10}. We select a norm in R^{10} as follows:

$$|(z_1, \ldots, z_{10})| = \max\Big\{|z_1|, |z_2| + |z_3|, |z_4| + |z_5|, |z_6| + |z_7|, |z_8| + |z_9|, |z_{10}|\Big\}.$$

Furthermore, let $\sigma(Q)$ denote the Lozinskii measure of Q with respect to the induced matrix norm $|\cdot|$ in R^{10}, defined as

$$\sigma(Q) = \lim_{h \to 0^+} \frac{|I + hQ| - 1}{h}.$$

The Lozinskii measure $\sigma(Q)$ can be estimated as follows (see [25]):

$$\sigma(Q(s, i_1, i_A, r_1, i_2)) \leq \sup\{g_1, g_2, g_3, g_4, g_5, g_6\},$$

where

$$g_1 = \sigma_1(Q_{11}) + |Q_{12}| + |Q_{13}| + |Q_{14}| + |Q_{15}| + |Q_{16}|, \; g_2 = \sigma_1(Q_{22}) + |Q_{21}| + |Q_{23}| + |Q_{24}| + |Q_{25}| + |Q_{26}|,$$
$$g_3 = \sigma_1(Q_{33}) + |Q_{31}| + |Q_{32}| + |Q_{34}| + |Q_{35}| + |Q_{36}|, \; g_4 = \sigma_1(Q_{44}) + |Q_{41}| + |Q_{42}| + |Q_{43}| + |Q_{45}| + |Q_{46}|,$$
$$g_5 = \sigma_1(Q_{55}) + |Q_{51}| + |Q_{52}| + |Q_{53}| + |Q_{54}| + |Q_{56}|, \; g_6 = \sigma_1(Q_{66}) + |Q_{61}| + |Q_{62}| + |Q_{63}| + |Q_{64}| + |Q_{65}|.$$

Let σ_1 denote the Lozinskii measure with respect to the l_1 norm, and $\left|Q_{ij}\right| (i \neq j, i, j = 1, 2, 3, 4, 5, 6)$ represents the matrix norm induced by the l_1 vector norm. To determine the value of g_i, we first compute

$$\sigma_1(Q_{11}) = \beta_1 s - \beta_1 i_1 - \beta_A i_A - (1 + \phi_1)\beta_2 i_2 - \eta_1 - 2\mu - \frac{i_1'}{i_1},$$
$$\sigma_1(Q_{22}) = \beta_A s - \beta_1 i_1 - \beta_A i_A - (1 + \phi_1)\beta_2 i_2 - 2\mu - \frac{i_1'}{i_1},$$
$$\sigma_1(Q_{33}) = \beta_1 s + \beta_A s - \eta_1 - \eta_A - 2\mu - \frac{i_A'}{i_A}, \quad \sigma_1(Q_{44}) = \beta_1 s - \eta_1 - 2\mu - \frac{i_A'}{i_A},$$
$$\sigma_1(Q_{55}) = \beta_A s - \eta_A - 2\mu - \frac{i_2'}{i_2}, \quad \sigma_1(Q_{66}) = (1 + \phi_1)\beta_2 s + \phi_2\beta_2 r_1 - \phi_2\beta_2 i_2 - \eta_2 - 2\mu - \frac{i_2'}{i_2},$$

and

$$|Q_{12}| = 0, \quad |Q_{13}| = \beta_A s, \quad |Q_{14}| = (1 + \phi_1)\beta_2 s, \quad |Q_{15}| = 0, \quad |Q_{16}| = 0,$$

$|Q_{21}| = \eta_1,\ |Q_{23}| < \max\{\beta_1 s, \phi_2\beta_2 r_1\},\ |Q_{24}| = \beta_1 s,\ |Q_{25}| < \max\{\beta_A s, (1+\phi_1)\beta_2 s\},\ |Q_{26}| = (1+\phi_1)\beta_2 s,$
$|Q_{31}| = \beta_A i_A, \quad |Q_{32}| < \max\{\beta_1 i_1, \phi_2\beta_2 i_2\}, \quad |Q_{34}| = \beta_1 s, \quad |Q_{35}| = \beta_A s, \quad |Q_{36}| = 0,$
$|Q_{41}| = (1+\phi_1)\beta_2 i_2, \quad |Q_{42}| = \beta_1 i_1, \quad |Q_{43}| < \max\{\beta_1 i_1, \eta_A\}, \quad |Q_{45}| = 0, \quad |Q_{46}| = 0,$
$|Q_{51}| = 0, \quad |Q_{52}| < \max\{(1+\phi_1)\beta_2 i_2, \beta_A i_A\}, \quad |Q_{53}| < \max\{\beta_A i_A, \eta_1\}, \quad |Q_{54}| = 0, \quad |Q_{56}| = 0,$
$|Q_{61}| = 0, \quad |Q_{62}| = (1+\phi_1)\beta_2 i_2, \quad |Q_{63}| = 0, \quad |Q_{64}| = \eta_1, \quad |Q_{65}| = \eta_A.$

Moreover, it follows from System (2.2) that

$$\frac{i_1'}{i_1} = \beta_1 s - (\eta_1 + \mu), \quad \frac{i_A'}{i_A} = \beta_A s - (\eta_A + \mu), \quad \frac{i_2'}{i_2} = (1+\phi_1)\beta_2 s + \phi_2\beta_2 r_1 - (\eta_2 + \mu).$$

Given

$$\bar{b} = \max\left\{\frac{\beta_1\Lambda}{\mu}, \frac{\beta_A\Lambda}{\mu}, \frac{(1+\phi_1)\beta_2\Lambda}{\mu}, \frac{\phi_2\beta_2\Lambda}{\mu}, \eta_1, \eta_A\right\},$$

we derive

$$g_1 < -\mu + \frac{(\beta_A + (1+\phi_1)\beta_2)\Lambda}{\mu}, \quad g_2 < -\mu + 2(\eta_1 + \bar{b}) + \frac{(\beta_A + (1+\phi_1)\beta_2)\Lambda}{\mu},$$
$$g_3 < -\mu + \bar{b} + \frac{(2\beta_1 + 2\beta_A)\Lambda}{\mu}, \quad g_4 < -\mu + \eta_A + \bar{b} + \frac{(2\beta_1 + (1+\phi_1)\beta_2)\Lambda}{\mu},$$
$$g_5 < -\mu + \eta_2 + 2\bar{b} + \frac{\beta_A\Lambda}{\mu}, \quad g_6 = -\mu + \eta_1 + \eta_A.$$

Let

$$\bar{c} = \Big\{\mu - \frac{(\beta_A + (1+\phi_1)\beta_2)\Lambda}{\mu}, \mu - 2(\bar{b} + \eta_1) - \frac{(\beta_A + (1+\phi_1)\beta_2)\Lambda}{\mu}, \mu - \bar{b} - \frac{(2\beta_1 + 2\beta_A)\Lambda}{\mu},$$
$$\mu - \bar{b} - \eta_A - \frac{(2\beta_1 + (1+\phi_1)\beta_2)\Lambda}{\mu}, \mu - 2\bar{b} - \eta_2 - \frac{\beta_A\Lambda}{\mu}, \mu - \eta_1 - \eta_A\Big\}.$$

From Condition (4.3), it follows that $\bar{c} > 0$ and

$$g_1 \le -\bar{c}, \quad g_2 \le -\bar{c}, \quad g_3 \le -\bar{c}, \quad g_4 \le -\bar{c}, \quad g_5 \le -\bar{c}, \quad g_6 \le -\bar{c}.$$

For every solution $(s(t), i_1(t), i_A(t), r_1(t), i_2(t))$ of System (2.2) with the initial value $(s(0), i_1(0), i_A(0), r_1(0), i_2(0)) \in \Gamma$, when $t > T$, we have

$$\frac{1}{t}\int_0^t g_1 ds \le -\bar{c},\ \frac{1}{t}\int_0^t g_2 ds \le -\bar{c},\ \frac{1}{t}\int_0^t g_3 ds \le -\bar{c},$$
$$\frac{1}{t}\int_0^t g_4 ds \le -\bar{c},\ \frac{1}{t}\int_0^t g_5 ds \le -\bar{c},\ \frac{1}{t}\int_0^t g_6 ds \le -\bar{c}.$$

Thus, it follows that

$$\frac{1}{t}\int_0^t \sigma(Q(s, i_1, i_A, r_1, i_2))ds \le \sup\{-\bar{c}, -\bar{c}, -\bar{c}, -\bar{c}, -\bar{c}, -\bar{c}\}.$$

Furthermore, this implies that

$$\overline{q} = \limsup_{t\to\infty} \sup_{x_0\in\Gamma} \frac{1}{t}\int_0^t \sigma(Q(x(s, x_0)))\, ds \le -\bar{c} < 0.$$

Therefore, the endemic equilibrium $\bar{E}$ of System (2.2) is globally asymptotically stable.

Theorem 4.7. *If the endemic equilibrium $\hat{E}$ exists and the system satisfies the condition*

$$\mu > \max\left\{2(\bar{b}+\eta_1)+\frac{(\beta_A+(1+\phi_1)\beta_2)\Lambda}{\mu}, \bar{b}+\frac{(2\beta_1+2\beta_A)\Lambda}{\mu}, \right.$$
$$\left. \bar{b}+\eta_A+\frac{(2\beta_1+(1+\phi_1)\beta_2)\Lambda}{\mu}, 2\bar{b}+\eta_2+\frac{\beta_A\Lambda}{\mu}, \eta_1+\eta_A\right\},$$

then System (2.2) *is globally asymptotically stable at $\hat{E}(\hat{s}, 0, \hat{i}_A, \hat{r}_1, \hat{i}_2)$.*

Proof. The proof follows a similar approach to Theorem 4.6.

Remark 4.1. *Condition* (4.3) *is not unique. Different choices of the matrix function $P(x)$ may lead to alternative sufficient conditions.*

4.3. Numerical simulations

In this section, we verify the theoretical results of System (2.2) through numerical simulations. During our analysis, it is recognized that the available data might be inadequate for precisely differentiating between ϕ_1 and ϕ_2. To simplify the model while focusing on the overall impact of the ADE effect, we adopt the assumption that $\phi_1 = \phi_2 = \phi$. The justification for the simplification $\phi_1 = \phi_2 = \phi$ is provided in Appendix B. Start by setting some parameters as follows: $\Lambda = 0.03$, $\mu = 0.02$, $\phi = 1.5$, $\eta_1 = 0.15$, $\eta_A = 0.1$, $\eta_2 = 0.2$, $\beta_1 = 0.06$, $\beta_A = 0.04$, and $\beta_2 = 0.03$. Figure 2 illustrates the six scenarios for the stability of the disease-free equilibrium, boundary equilibria, and endemic equilibria.

The results indicate that if $R_1 < 1$, $R_A < 1$, and $R_2 < 1$, then the disease-free equilibrium E_0 is stable, and both strains disappear (Figure 2(a)). If $R_1 > 1$, $R_A < 1$, $R_2 < 1$, and the condition $\frac{\mu}{\eta_A+\mu}R_1 > 1$ in Theorem 4.2 is satisfied, then the single-strain infection equilibrium E_1 is stable. In this case, symptomatic infections of Strain 1 persist stably, while asymptomatic infections of Strain 1 and infections of Strain 2 disappear (Figure 2(b)). If $R_1 < 1$, $R_A > 1$, $R_2 < 1$, and the condition $\frac{\mu}{\eta_1+\mu}R_A > 1$ in Theorem 4.3 is satisfied, then the single-strain infection equilibrium E_A is stable. Here, asymptomatic infections of Strain 1 persist stably, while symptomatic infections of Strain 1 and infections of Strain 2 disappear (Figure 2(c)). If $R_1 < 1$, $R_A < 1$, $R_2 > 1$, and the conditions $\frac{\mu}{\eta_1+\mu}R_2 > 1$ and $\frac{\mu}{\eta_A+\mu}R_2 > 1$ in Theorem 4.4 are satisfied, then the single-strain infection equilibrium E_2 is stable. In this scenario, Strain 2 persists stably, while symptomatic and asymptomatic infections of Strain 1 disappear (Figure 2(d)). If $R_1 > 1$, $R_A < 1$, $R_2 > 1$, and the condition $\widetilde{R}_1 < R_2 < R_1$ in Theorem 4.5 are satisfied, then the dual-strain infection equilibrium $\bar{E}$ is stable. In this case, symptomatic infections of Strain 1 and infections of Strain 2 persist stably, while asymptomatic infections of Strain 1 disappear (Figure 2(e)). If $R_1 < 1$, $R_A > 1$, $R_2 > 1$, and the condition $\widetilde{R}_A < R_2 < R_A$ in Theorem 4.5 are satisfied, then the dual-strain infection equilibrium $\hat{E}$ is stable. Here, asymptomatic infections of Strain 1 and infections of Strain 2 persist stably, while symptomatic infections of Strain 1 disappear (Figure 2(f)).

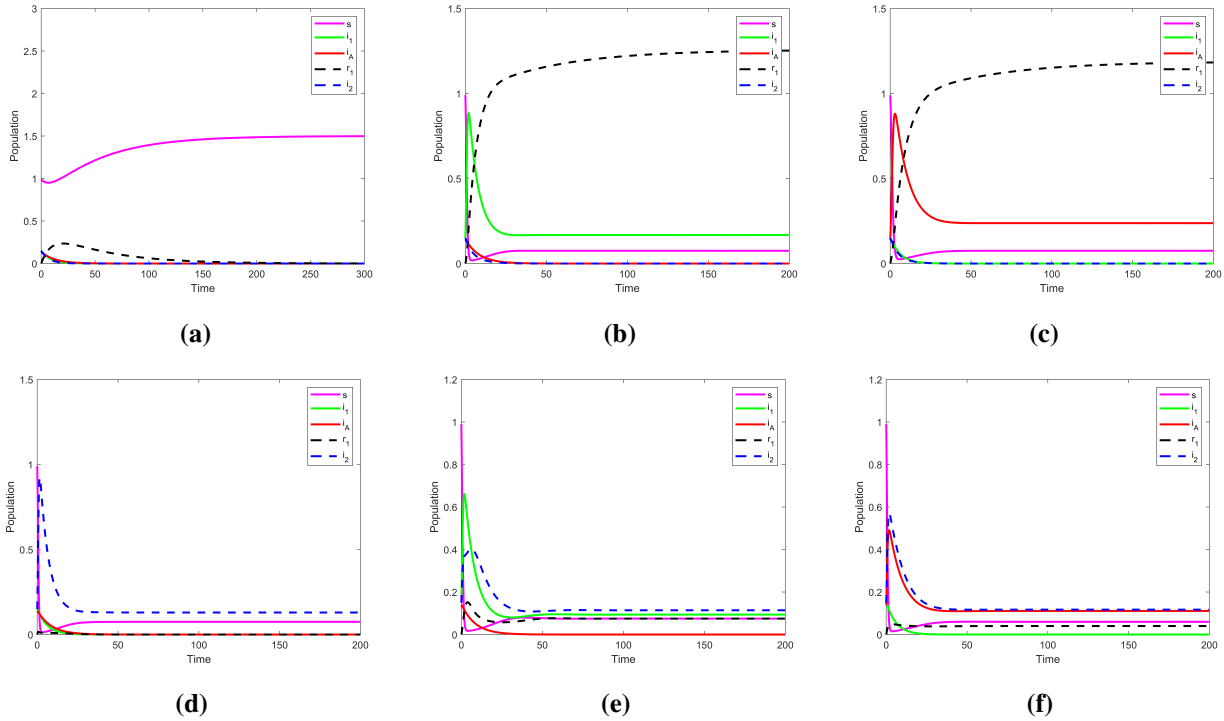

Figure 2. Stability analysis of the system. (a) E_0 is stable when $\beta_1 = 0.06, \beta_A = 0.04$, and $\beta_2 = 0.03$, with $R_1 = 0.5 < 1, R_A = 0.5 < 1$, and $R_2 = 0.5 < 1$. (b) E_1 is stable when $\beta_1 = 2.27, \beta_A = 0.04$, and $\beta_2 = 0.03$, with $R_1 = 20 > 1, R_A = 0.5 < 1$, and $R_2 = 0.5 < 1$. (c) E_A is stable when $\beta_1 = 0.06, \beta_A = 1.6$, and $\beta_2 = 0.03$, with $R_1 = 0.5 < 1, R_A = 20 > 1$, and $R_2 = 0.5 < 1$. (d) E_2 is stable when $\beta_1 = 0.06, \beta_A = 0.04$, and $\beta_2 = 1.17$, with $R_1 = 0.5 < 1, R_A = 0.5 < 1$, and $R_2 = 20 > 1$. (e) $\bar{E}$ is stable when $\beta_1 = 2.27, \beta_A = 0.04$, and $\beta_2 = 0.59$, with $R_1 = 20 > 1, R_A = 0.5 < 1$, and $R_2 = 10 > 1$. (f) $\hat{E}$ is stable when $\beta_1 = 0.06, \beta_A = 2.00$, and $\beta_2 = 0.88$, with $R_1 = 0.5 < 1, R_A = 25 > 1$, and $R_2 = 15 > 1$.

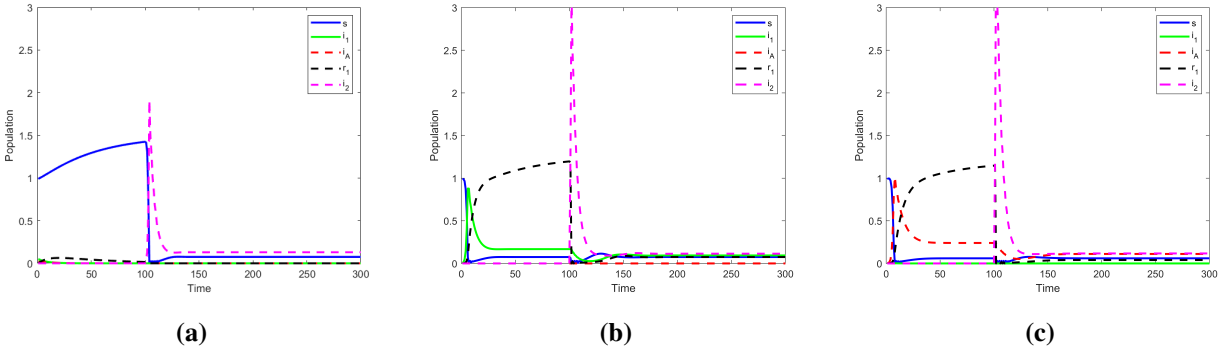

Figure 3. Stability analysis of the system. (a) E_2 is stable when $\beta_1 = 0.06, \beta_A = 0.04$, and $\beta_2 = 1.17$, with $R_1 = 0.5 < 1, R_A = 0.5 < 1$, and $R_2 = 20 > 1$. (b) $\bar{E}$ is stable when $\beta_1 = 2.27, \beta_A = 0.04$, and $\beta_2 = 0.59$, with $R_1 = 20 > 1, R_A = 0.5 < 1$, and $R_2 = 10 > 1$. (c) $\hat{E}$ is stable when $\beta_1 = 0.06, \beta_A = 2.00$, and $\beta_2 = 0.88$, with $R_1 = 0.5 < 1, R_A = 25 > 1$, and $R_2 = 15 > 1$.

Additionally, Figure 3 illustrates the stability diagram under the assumption that a new strain emerges at $t = 100$. The peak proportion of infections by the new strain is significantly higher in Figure 3(b) than in Figure 3(a). This observation precisely reflects the impact of the ADE effect on viral transmission. Specifically, antibodies generated from prior infections with a virus may enhance the infectivity of a new similar but distinct virus, rather than suppressing the infection. Similarly, the influence of the ADE effect on viral transmission is also evident, as the peak proportion of the new strain's infections in Figure 3(c) exceeds that in Figure 3(a).

5. A case study: Influenza pandemic in Geneva, Switzerland

5.1. Data sources and parameter estimation

In this section, we utilize the daily epidemiological data of the Spanish influenza pandemic in Geneva, Switzerland, from July 1918 to February 1919 [26]. For this study, Week 27 of 1918 is selected as the first observation day, and the analysis focuses on the weekly reported cumulative cases in Geneva between July 1 and December 15, 1918.

One of our challenges is the lack of detailed data on the simultaneous circulation of both viral strains. However, existing epidemiological studies [17, 27] demonstrate that influenza typically exhibits seasonal patterns, with different strains potentially dominating across seasons. An analysis of the influenza surveillance data from Geneva [26] reveals two infection peaks between July 1 and December 15, 1918, corresponding to the summer and autumn waves. According to reports [28], the pandemic occurred in two waves—summer and autumn—with the autumn wave demonstrating significantly higher mortality rates. On the basis of this observation, we assume that the summer wave was primarily driven by Strain 1, while the autumn wave may have involved the cocirculation of both strains with an ADE effect, predominantly dominated by Strain 2. We perform a piecewise fitting of the data using the least squares method. The results of the fitting are shown in Figure 4. The parameter values, which include both the given and fitted values, are provided in Table 2. The goodness-of-fit R^2 for the two segments is 0.9776 and 0.9842, respectively.

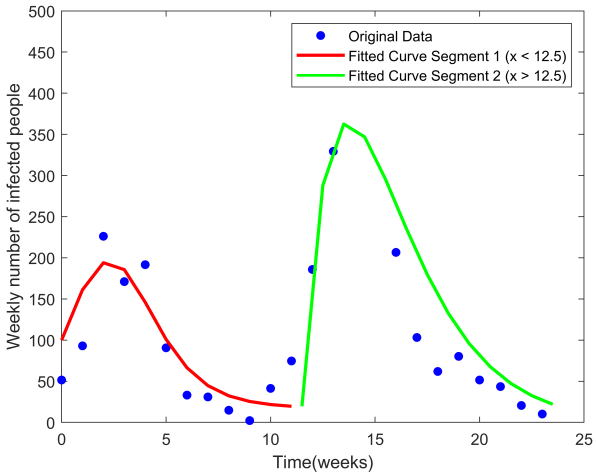

Figure 4. Results of data fitting for the 1918 influenza pandemic in Geneva, Switzerland.

Table 2. Parameter values.

Parameters	Values	Sources	95% CI
Λ	0.02	Fitted	[0.0185, 0.0212]
ϕ	1.13	Fitted	[1.0500, 1.2100]
β_1	0.67	Fitted	[0.6100, 0.7300]
β_A	0.69	Fitted	[0.6300, 0.7500]
β_2	0.66	Fitted	[0.5900, 0.7200]
η_1	[0.09, 0.5]	[29]	–
η_A	0.10	Assumed	–
η_2	[0.09, 0.5]	[29]	–
μ	0.00005	[30]	–

5.2. Impact of ADE on cumulative cases in Geneva, Switzerland

To further investigate the impact of the ADE factor on the infection dynamics during the autumn wave of the influenza pandemic in Geneva, we examine the effects of varying ADE factors on the autumn transmission. The result is presented in Figure 5.

As shown in Figure 5, if $\phi = 1.5$, indicating that the probability of infection with the autumn wave's influenza virus is 1.5 times higher than before, the cumulative number of influenza cases in Geneva, Switzerland, by the 15th week of 1918 would reach 362. If the probability of infection increases to 2.5 times the original level, the cumulative number of cases by the 15th week would rise to 427. As ϕ increases, the peak cumulative number of influenza cases in Geneva also rises progressively. Clearly, a higher ADE factor ϕ demonstrates a stronger cumulative effect.

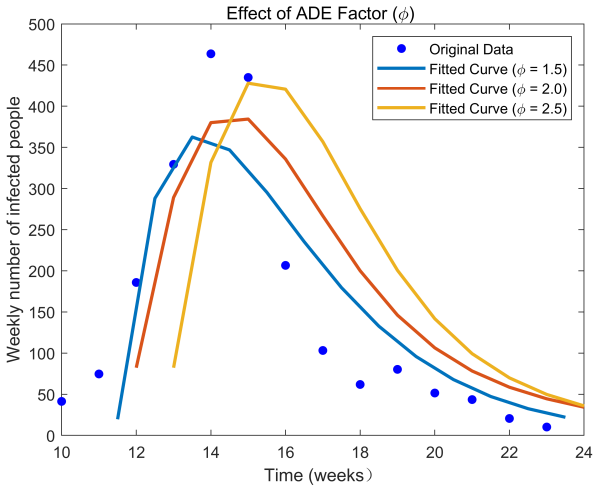

Figure 5. Impact of the ADE factor ϕ on the 1918 autumn influenza wave in Geneva.

6. Optimal control analysis and numerical simulation incorporating ADE risk

6.1. Analysis of optimal control

Effectively controlling and treating infectious diseases poses significant challenges in resource-limited settings [31]. This section examines influenza control strategies by balancing control efficacy against resource constraints. In particular, to address the additional risks posed by vaccination-induced ADE, our analytical framework explicitly incorporates the evaluation of ADE risk and its trade-off with epidemic control outcomes.

There are three common measures for preventing influenza: Vaccination, personal daily protection, and antiviral treatment [2]. For instance, in [30], the authors developed a multiscale immune influenza model that incorporates both antiviral treatment and vaccination. The findings indicate that while antiviral treatment can significantly reduce an individual's viral load, it may also increase potential risks at the population level.

Building upon prior analyses and practical considerations, we propose two categories of control measures—pharmaceutical treatments and behavioral interventions (e.g., promoting mask-wearing, maintaining social distancing, and encouraging voluntary vaccination)—to effectively mitigate disease transmission. The control variables primarily act on the parameters associated with each control measure.

Specifically, u_1 represents the control variable for pharmaceutical treatment targeting the original strain, while u_2 corresponds to the control variable for pharmaceutical treatment targeting the new strain. In addition, u_3 denotes the control variable associated with behavioral intervention measures, reflecting the intensity of non-pharmaceutical interventions, and u_4 represents the control variable for vaccination targeting the original strain, which works in synergy with u_3 to reduce the risk of infection with the original strain. Similarly, u_5 denotes the control variable for vaccination targeting the new strain, collaborating with u_3 to lower the risk of infection with the new strain. Notably, pharmaceutical treatments are typically administered to symptomatic patients, as asymptomatic individuals are less likely to receive such treatments. Consequently, the increase in recovery rates applies only to symptomatic individuals infected with the original strain and individuals infected with the new strain.

Assume that $\bar{u}_i \in (0, 1)$ exists such that $0 \leq u_i(t) \leq \bar{u}_i < 1, i = 1, 2, 3, 4, 5$. Within a fixed time interval $[0, t_f]$ for $t_f > 0$, the feasible decision space or constraint set is defined as

$$U = \{u_i(t) | 0 \leq u_i(t) \leq \bar{u}_i, 0 \leq t \leq t_f, u_i(t) \text{ is Lebesgue measurable}, i = 1, 2, 3, 4, 5\}.$$

The primary objective of this study is to minimize both the cost associated with pharmaceutical treatment and behavioral interventions and the economic losses caused by the treatment of infected individuals. Within the time interval $[0, t_f]$, these costs are respectively denoted as

$$\int_0^{t_f} B_1 i_1(t) u_1(t) dt, \int_0^{t_f} B_2 i_2(t) u_2(t) dt, \int_0^{t_f} B_3 s(t) u_3(t) dt,$$
$$\int_0^{t_f} B_4 s(t) u_4(t) dt, \int_0^{t_f} B_4 s(t) u_5(t) dt, \int_0^{t_f} (D_1(i_1(t) + i_A(t)) + D_2 i_2(t)) dt.$$

Here, B_1 represents the cost of pharmaceutical treatment for the original strain. B_2 denotes the cost of pharmaceutical treatment for the new strain. B_3 is the cost of implementing behavioral interventions

(nonpharmacological interventions). B_4 is the cost of implementing the behavioral intervention (vaccination). D_1 and D_2, respectively, represent the healthcare resource costs per case of influenza caused by the original strain and the new strain.

In addition to the aforementioned cost objectives, our framework explicitly incorporates ADE risk aversion. Based on the immunological mechanisms of ADE, this risk arises from four distinct scenarios: (i) Homologous exogenous ADE in individuals vaccinated with Strain 1 upon reinfection with Strain 1 corresponds to $u_4(t)i_1(t)$, (ii) heterologous exogenous ADE in individuals vaccinated with Strain 1 upon infection with Strain 2 corresponds to $u_4(t)i_2(t)$, (iii) homologous exogenous ADE in individuals vaccinated with Strain 2 upon reinfection with Strain 2 corresponds to $u_5(t)i_2(t)$, and (iv) endogenous ADE in individuals recovered from Strain 1 upon subsequent infection with Strain 2 corresponds to $r_1(t)i_2(t)$. To account for these risks, we introduce the following ADE risk penalty term in the objective function:

$$P(t) = \alpha(u_4(t)i_1(t) + u_4(t)i_2(t) + u_5(t)i_2(t) + r_1(t)i_2(t)),$$

to preserve the convexity of the penalty function, using the arithmetic mean-geometric mean (AM-GM) inequality, for any feasible $u_4(t), u_5(t), i_1(t), i_2(t), r_1(t) > 0$, we have

$$P(t) \leq \frac{\alpha}{2}(2u_4^2(t) + u_5^2(t) + i_1^2(t) + 3i_2^2(t) + r_1^2(t)).$$

Here, the risk-weighting coefficient α represents the decision-maker's degree of aversion to the risk that ADE may exacerbate illness during an epidemic. Due to the current lack of precise quantitative comparisons among different ADE risk sources, a conservative assumption is adopted to avoid overestimating the impact of specific risk sources: All risk sources share the same risk coefficient. Considering that $r_1(t)$, as a state variable, responds to control inputs with a lag, its weight is appropriately reduced. The final convex penalty function is given by

$$\bar{P}(t) = \alpha(u_4^2(t) + 0.5u_5^2(t) + 0.5i_1^2(t) + 1.5i_2^2(t) + 0.1r_1^2(t)).$$

Based on the assumptions above, the optimal control problem can be formulated as follows:

$$\begin{cases} \dfrac{ds}{dt} = \Lambda - (1 - u_3(t) - u_4(t))\beta_1 s i_1 - (1 - u_3(t) - u_4(t))\beta_A s i_A - (1 - u_3(t) - u_5(t))(1 + \phi)\beta_2 s i_2 - \mu s, \\ \dfrac{di_1}{dt} = (1 - u_3(t) - u_4(t))\beta_1 s i_1 - (1 + u_1(t))\eta_1 i_1 - \mu i_1, \\ \dfrac{di_A}{dt} = (1 - u_3(t) - u_4(t))\beta_A s i_A - \eta_A i_A - \mu i_A, \\ \dfrac{dr_1}{dt} = (1 + u_1(t))\eta_1 i_1 + \eta_A i_A - (1 - u_3(t) - u_5(t))\phi\beta_2 r_1 i_2 - \mu r_1, \\ \dfrac{di_2}{dt} = (1 - u_3(t) - u_5(t))(1 + \phi)\beta_2 s i_2 + (1 - u_3(t) - u_5(t))\phi\beta_2 r_1 i_2 - (1 + u_2(t))\eta_2 i_2 - \mu i_2, \\ \dfrac{dr_2}{dt} = (1 + u_2(t))\eta_2 i_2 - \mu r_2, \end{cases}$$

with the initial conditions

$$\begin{aligned} 0 \leq s(0) \leq L, \quad 0 \leq i_1(0) \leq L, \quad 0 \leq i_A(0) \leq L, \\ 0 \leq r_1(0) \leq L, \quad 0 \leq i_2(0) \leq L, \quad 0 \leq r_2(0) \leq L, \end{aligned}$$

where L is the positive constant.

Subsequently, the vector-valued optimization problem is reformulated as a scalar quadratic optimization problem through a weighted sum approach, yielding the following unique objective function:

$$J(u_1(t), u_2(t), u_3(t)) = \int_0^{t_f} [\omega_1(B_1 i_1(t)u_1(t))^2 + \omega_2(B_2 i_2(t)u_2(t))^2 + \omega_3(B_3 s(t)u_3(t))^2$$
$$+ \omega_4((B_4 s(t)u_4(t))^2 + (B_4 s(t)u_5(t))^2) + \omega_5((D_1(i_1(t) + i_A(t)))^2 + (D_2 i_2(t))^2) + \bar{P}(t)]dt.$$

Theorem 6.1. *There is a set of $u_1(t), u_2(t), u_3(t), u_4(t)$, and $u_5(t)$, so that*

$$J(u_1^*(t), u_2^*(t), u_3^*(t), u_4^*(t), u_5^*(t)) = \min J(u_1(t), u_2(t), u_3(t), u_4(t), u_5(t)).$$

The optimal control expressions are as follows:

$$u_1^*(t) = \max\{\min\{\overline{u}_1, \frac{(\lambda_{i_1} - \lambda_{r_1})\eta_1}{2\omega_1 B_1^2 i_1(t)}\}, 0\},\ u_2^*(t) = \max\{\min\{\overline{u}_2, \frac{(\lambda_{i_2} - \lambda_{r_2})\eta_2}{2\omega_2 B_2^2 i_2(t)}\}, 0\},$$
$$u_3^*(t) = \max\{\min\{\overline{u}_3, \frac{\Psi_3(t)}{2\omega_3 B_3^2 s^2(t)}\}, 0\},\ u_4^*(t) = \max\{\min\{\overline{u}_4, \frac{\Psi_4(t)}{2\omega_4 B_4^2 s^2(t) + 2\alpha}\}, 0\},$$
$$u_5^*(t) = \max\{\min\{\overline{u}_5, \frac{\Psi_5(t)}{2\omega_4 B_4^2 s^2(t) + \alpha}\}, 0\},$$

where

$$\Psi_3(t) = (\lambda_{i_1} - \lambda_s)\beta_1 s i_1(t) + (\lambda_{i_A} - \lambda_s)\beta_A s i_A(t) + (\lambda_{i_2} - \lambda_s)(1 + \phi)\beta_2 s i_2(t) + (\lambda_{i_2} - \lambda_{r_1})\phi\beta_2 r_1 i_2(t),$$
$$\Psi_4(t) = (\lambda_{i_1} - \lambda_s)\beta_1 s i_1(t) + (\lambda_{i_A} - \lambda_s)\beta_A s i_A(t),$$
$$\Psi_5(t) = (\lambda_{i_2} - \lambda_s)(1 + \phi)\beta_2 s i_2(t) + (\lambda_{i_2} - \lambda_{r_1})\phi\beta_2 r_1 i_2(t).$$

Proof. According to Pontryagin's extreme value principle, the Hamiltonian function is defined as follows:

$$\begin{aligned} H = {} & \omega_1(B_1 i_1(t)u_1(t))^2 + \omega_2(B_2 i_2(t)u_2(t))^2 + \omega_3(B_3 s(t)u_3(t))^2 + \omega_4[(B_4 s(t)u_4(t))^2 + (B_4 s(t)u_5(t))^2] \\ & + \omega_5[(D_1(i_1(t) + i_A(t)))^2 + (D_2 i_2(t))^2] + \bar{P}(t) \\ & + \lambda_s[\Lambda - (1 - u_3(t) - u_4(t))\beta_1 s i_1 - (1 - u_3(t) - u_4(t))\beta_A s i_A - (1 - u_3(t) - u_5(t))(1 + \phi)\beta_2 s i_2 - \mu s] \\ & + \lambda_{i_1}[(1 - u_3(t) - u_4(t))\beta_1 s i_1 - (1 + u_1(t))\eta_1 i_1 - \mu i_1] \\ & + \lambda_{i_A}[(1 - u_3(t) - u_4(t))\beta_A s i_A - \eta_A i_A - \mu i_A] \\ & + \lambda_{r_1}[(1 + u_1(t))\eta_1 i_1 + \eta_A i_A - (1 - u_3(t) - u_5(t))\phi\beta_2 r_1 i_2 - \mu r_1] \\ & + \lambda_{i_2}[(1 - u_3(t) - u_5(t))(1 + \phi)\beta_2 s i_2 + (1 - u_3(t) - u_5(t))\phi\beta_2 r_1 i_2 - (1 + u_2(t))\eta_2 i_2 - \mu i_2] \\ & + \lambda_{r_2}[(1 + u_2(t))\eta_2 i_2 - \mu r_2], \end{aligned}$$

where λ_m denotes the adjoint variable corresponding to the adjoint equation given in Appendix C.

Therefore, the optimal control strategy $(u_1^*(t), u_2^*(t), u_3^*(t), u_4^*(t), u_5^*(t))$ can be solved by the following optimality conditions:

$$\frac{\partial H}{\partial u_1(t)}|_{(u_1^*(t), u_2^*(t), u_3^*(t), u_4^*(t), u_5^*(t))} = 0, \quad \frac{\partial H}{\partial u_2(t)}|_{(u_1^*(t), u_2^*(t), u_3^*(t), u_4^*(t), u_5^*(t))} = 0,$$
$$\frac{\partial H}{\partial u_3(t)}|_{(u_1^*(t), u_2^*(t), u_3^*(t), u_4^*(t), u_5^*(t))} = 0, \quad \frac{\partial H}{\partial u_4(t)}|_{(u_1^*(t), u_2^*(t), u_3^*(t), u_4^*(t), u_5^*(t))} = 0,$$
$$\frac{\partial H}{\partial u_5(t)}|_{(u_1^*(t), u_2^*(t), u_3^*(t), u_4^*(t), u_5^*(t))} = 0.$$

The proof is complete.

6.2. *Numerical simulation of optimal control*

In this section, we use the forward-backward Runge-Kutta method [32] to compute the optimal solution. Numerical simulations are conducted to validate the optimal control outcomes, thereby assessing the impact of optimal control strategies on the epidemic's dynamics. According to references [30,33], the weekly pharmaceutical treatment costs for influenza cases caused by the original strain and the new strain are approximately \$120 ($B_1 = 120$) per person and \$130 ($B_2 = 130$) per person, respectively. The weekly healthcare resource costs for influenza cases associated with the original strain and the new strain are approximately \$150 ($D_1 = 150$) per person and \$250 ($D_2 = 250$) per person, respectively. Additionally, the cost of implementing behavioral interventions is estimated to be approximately \$5 ($B_3 = 5$) per person per week. Furthermore, according to reference [34], assuming a six-month protection period for the influenza vaccine, the average weekly vaccination cost is approximately \$0.38 ($B_4 = 0.38$) per person.

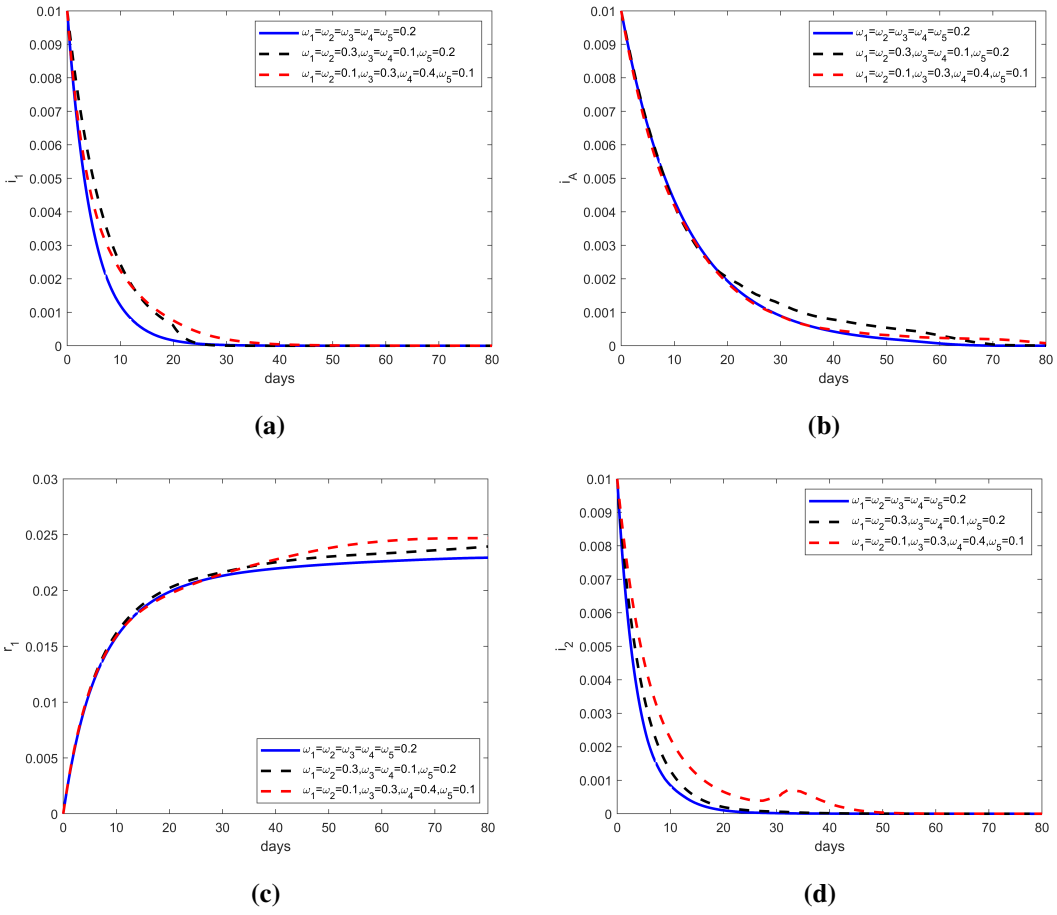

Figure 6. The trends of i_1, i_A, r_1, and i_2 under different weight coefficient configurations.

6.2.1. Without ADE risk

In conventional control studies, ADE risk is typically neglected (i.e., $\alpha = 0$). Assume three weighting schemes for intervention costs: (i) Balanced control ($\omega_1 = \omega_2 = \omega_3 = \omega_4 = \omega_5 = 0.2$), (ii) prioritized control of pharmaceutical treatment costs ($\omega_1 = \omega_2 = 0.3$, $\omega_3 = \omega_4 = 0.1$, $\omega_5 = 0.2$),

and (iii) prioritized control of behavioral intervention costs ($\omega_1 = \omega_2 = 0.1$, $\omega_3 = 0.3$, $\omega_4 = 0.4$, $\omega_5 = 0.1$). Figure 6 compares the control outcomes under these three weighting schemes. Numerical simulations indicate that under all three schemes, both the proportions of symptomatic individuals (i_1) and asymptomatic carriers (i_A) of the original strain demonstrate a rapid decline before eventually stabilizing. In particular, the control strategy with balanced weights demonstrates superior overall performance, achieving a better trade-off between control cost and epidemic scale.

Notably, Figure 7 compares influenza case counts in Geneva, Switzerland, before and after implementing the control strategy with balanced weighting coefficients ($\omega_1 = \omega_2 = \omega_3 = \omega_4 = \omega_5 = 0.2$). Numerical simulations demonstrate that the optimal control strategy effectively suppresses the growth of the infected proportion, ultimately maintaining the epidemic at low endemic levels.

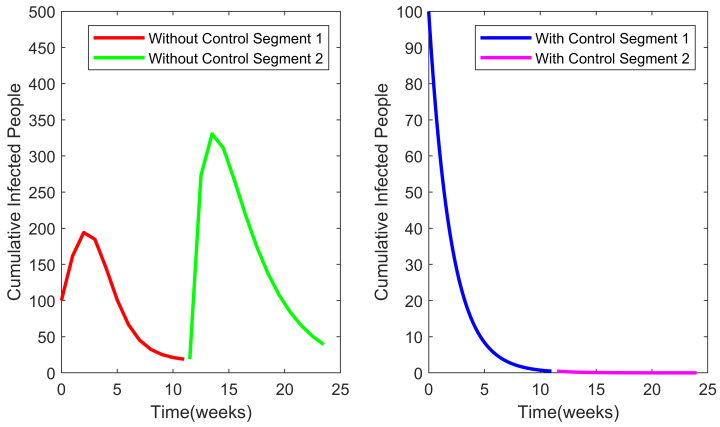

Figure 7. Comparative dynamics of influenza's transmission in Geneva, Switzerland, under uncontrolled and optimally controlled scenarios.

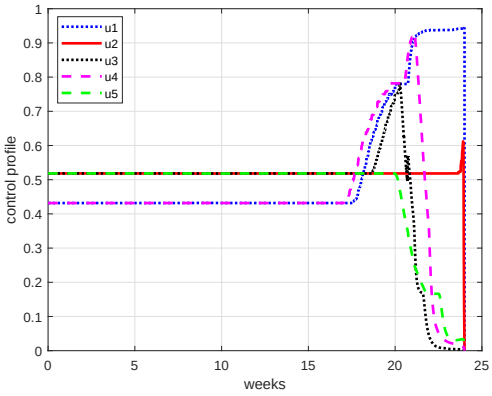

Figure 8. Optimal control strategy u_1, u_2, u_3, u_4, and u_5.

Additionally, Figure 8 shows the time-varying control profile under the balanced weights. The effective implementation of behavioral intervention measures (maintaining an intensity of approximately 51% in the first 17 weeks and increasing to 79% by Week 20) serves as a critical enabler of this control strategy, reducing the demand for pharmaceutical treatment resources to some extent. The results further show that after Week 17, the optimal control strategy substantially increases the

allocation to antiviral treatment and vaccination against the original strain. However, this increase in vaccination effort heightens the risk of ADE, marking a strategic shift in epidemic control from minimizing transmission alone to a new phase that explicitly accounts for immunological safety.

6.2.2. With ADE risk

The selection of the ADE risk weighting coefficient α depends on multiple factors, including the tolerable burden of vaccine-associated severe cases, the trade-off between population-level protection and individual risk, heterogeneity across patient populations, the epidemic phase, and vaccine safety profiles. If the decision-maker adheres to a "safety first" principle, α takes a larger value; if containing transmission is deemed to be more urgent, α is set to a smaller value. By varying the risk weight α, we derive the Pareto frontier between infection control and ADE risk. Each value of α corresponds to a point on this frontier, representing a specific risk preference (see Table 3 and Figure 9).

Table 3. Performance of optimal strategies under varying α.

α	Total infections	Total vaccinations	Mean vaccination rate	ADE risk	Strategy description
0.0	202.58	16130.59	0.9601	2.50	Baseline (ADE neglected)
1.0	206.24	15377.67	0.9153	1.67	Low aversion
2.0	207.24	15349.02	0.9136	1.25	Recommended strategy
3.0	208.06	15330.51	0.9125	1.00	Moderate aversion
4.0	208.66	15320.49	0.9119	0.83	Intermediate aversion
5.0	209.61	15308.43	0.9112	0.71	Conservative strategy
7.0	210.16	15302.80	0.9108	0.56	High aversion
10.0	211.21	15286.33	0.9098	0.42	Extreme aversion

Table 3 presents key performance metrics of the vaccination strategy as the ADE risk-aversion coefficient α varies from 0 to 10. The metrics are defined as follows: Total infections = $\int_0^{t_f}(i_1(t) + i_A(t) + i_2(t))\,dt$, total vaccinations = $\int_0^{t_f}(u_4(t) + u_5(t))\,dt$, mean vaccination rate = $\frac{1}{t_f}\int_0^{t_f}(u_4(t) + u_5(t))\,dt$, and ADE risk = $\int_0^{t_f}(u_4(t)i_1(t) + u_4(t)i_2(t) + u_5(t)i_2(t) + r_1(t)i_2(t))\,dt$. When the ADE risk is completely neglected ($\alpha = 0$), the system adopts an aggressive vaccination strategy, achieving the lowest number of infections (202.58) but the highest ADE risk index (2.50). As α increases, the strategy shifts toward conservatism: Total vaccinations decrease by 5.0%, the mean vaccination rate drops from 0.9601 to 0.9098, and ADE risk is significantly reduced by 83% to 0.42, while infections increase only marginally by 4.3% to 211.21. The trade-off curve in Figure 9 reveals a nonlinear relationship between infection control and ADE risk aversion. Within the interval $\alpha \in [0, 2]$, each unit of increase in α reduces the ADE risk by 0.63 at the cost of only 2.3 additional infections, yielding a benefit-cost ratio of 0.27. For $\alpha > 2$, the marginal benefit diminishes sharply: Increasing α from 2 to 10 reduces the ADE risk by merely an additional 0.83 while increasing infections by 4.0, lowering the benefit-cost ratio to 0.21. Overall, the strategy with $\alpha = 2.0$ demonstrates the most balanced performance, reducing the ADE risk by 50% at the cost of only a 2.3% increase in infections compared with the $\alpha = 0$ scenario.

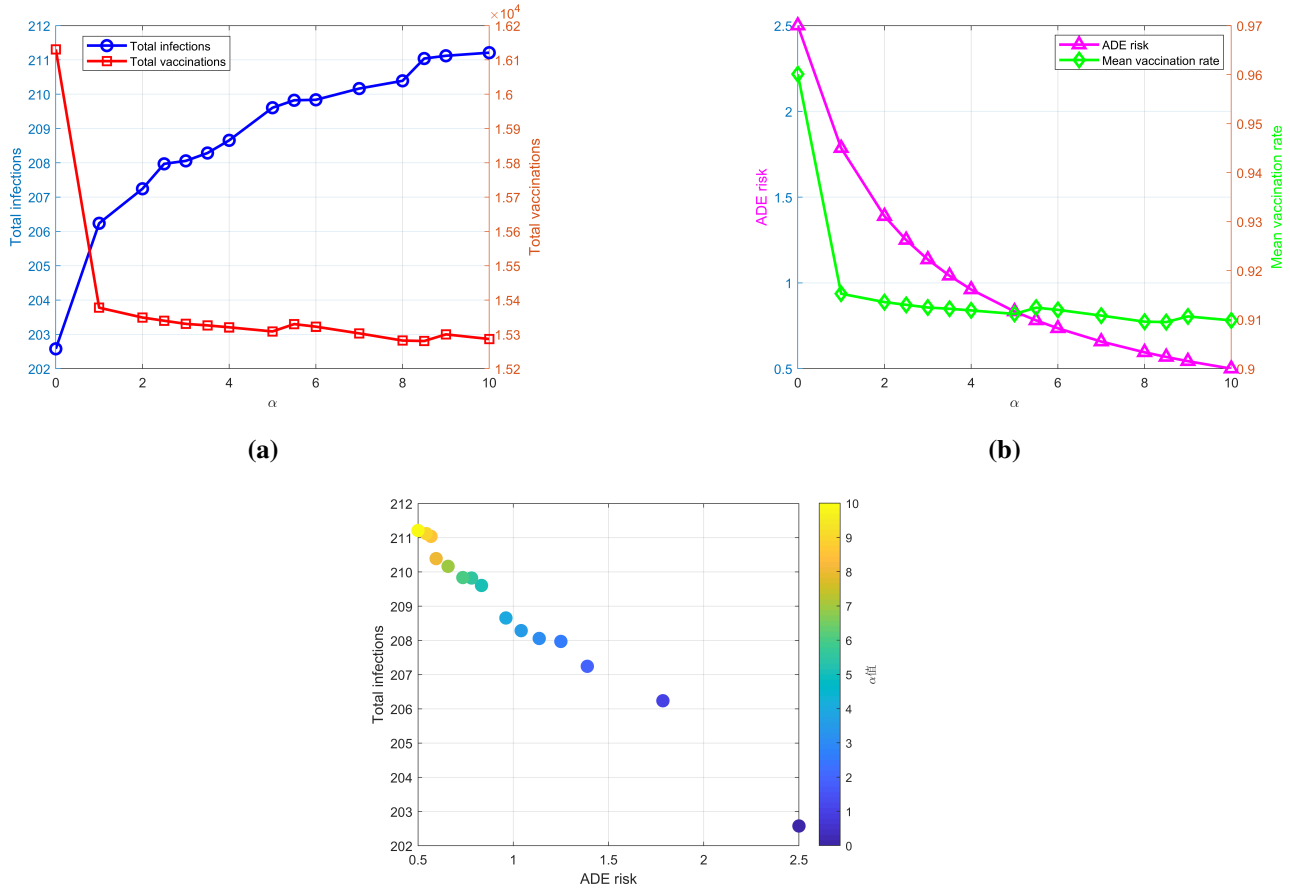

Figure 9. Impact of the ADE risk's weight on key outcomes and trade-offs. (a) Total infections and total vaccinations versus the ADE risk's weight. (b) The ADE risk index and mean vaccination rate versus the ADE risk's weight. (c) Trade-off between the ADE risk index and infection burden.

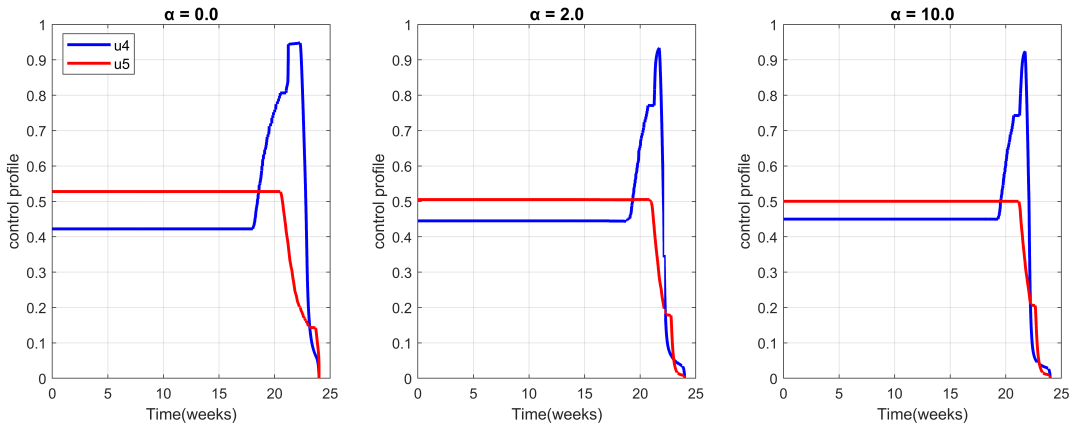

Figure 10. Temporal evolution of u_4 and u_5 under different values of α ($\alpha = 0, 2, 10$).

Figure 10 shows the temporal evolution of vaccination strategies for the original strain (u_4) and the new strain (u_5) under three different ADE risk weights. A comparison reveals that despite substantial variation in the ADE risk-aversion coefficient α over a wide range (0–10), the optimal vaccination strategies exhibit a consistent temporal structure, displaying similar patterns over time. This indicates that within the established two-strain epidemic dynamic framework, a dominant optimal vaccination rhythm exists, and the demand for risk aversion is primarily achieved by fine-tuning this fundamental pattern.

7. Conclusions and discussion

This study systematically investigates the complex role of ADE in influenza transmission by developing a two-strain transmission model that explicitly incorporates ADE effects. The model integrates ADE effects driven jointly by endogenous factors (the host's immune status) and exogenous factors (viral cross-reactivity), while appllying threshold theory to establish the existence and stability conditions of various equilibrium states. Dynamic analysis reveals that the system's evolutionary trajectory (see Table 4) is jointly determined by three transmission thresholds: The symptomatic transmission threshold of the original strain (R_1), the asymptomatic transmission threshold (R_A), and the transmission threshold of the new strain (R_2).

Therefore

$$\widetilde{R}_1 = \frac{\beta_1 \Lambda}{\mu(\mu + \eta_1 + \eta_1(R_1 - 1)\frac{\phi_2}{1+\phi_1})},$$

and

$$\widetilde{R}_A = \frac{\beta_A \Lambda}{\mu(\mu + \eta_A + \eta_A(R_A - 1)\frac{\phi_2}{1+\phi_1})}.$$

Increasing the exogenous ADE risk lowers these two thresholds, shifting the system from stable boundary equilibria to stable coexistence equilibria. In contrast, a higher endogenous ADE risk eliminates coexistence and stabilizes boundary equilibria, resulting in the eventual extinction of the original strain. In our case study, numerical simulations based on historical data from the 1918 Spanish influenza pandemic in Geneva, Switzerland, demonstrated ADE's pivotal role in driving the secondary outbreak in autumn. By enhancing the new strain's infectivity, ADE significantly increased the cumulative number of cases by approximately 86.8% relative to the scenario without ADE.

Specifically, this paper applies a multiobjective Pareto optimization framework to influenza control under ADE risk. By parameterizing the Pareto frontier via the risk-weighting coefficient α, we quantify the trade-off between infection control and safety. The results show the following.

1) In the absence of risk aversion ($\alpha = 0$), under resource-limited conditions, an integrated intervention strategy centered on drug therapy and behavioral modifications (e.g., mask-wearing, social distancing, and voluntary vaccination) can reduce the peak infection rate by approximately 94.7%, outperforming a drug-only strategy.

2) As the risk aversion coefficient α increases from 0 to 10, the ADE risk decreases by 83% at the cost of a 4.3% rise in infections—a typical Pareto trade-off. The interval $\alpha \in [1, 3]$ delivers the optimal benefit-cost ratio. In particular, the strategy with $\alpha = 2$ achieves a 50% reduction in the ADE risk with only a 2.3% increase in infections, representing the best balance between risk and benefit.

Furthermore, comparative analysis reveals that the structure of the optimal control strategy is insensitive to changes in the risk aversion coefficient. This provides a foundational policy blueprint for public health decision-makers, who can fine-tune the strategy according to specific risk assessments without concern for drastic strategic shifts.

Table 4. Existence and stability of equilibria for System (2.2).

Equilibria	Existence conditions	Local stability conditions	Global stability conditions
E_0	Always exists	$R_0 = \max\{R_1, R_A, R_2\} < 1$	$R_0 = \max\{R_1, R_A, R_2\} < 1$
		$R_1 > 1$	$R_1 > 1$
E_1	$R_1 > 1$	$R_1 > R_A$	$R_1 > \widetilde{\widetilde{R}}_A > R_A$
		$R_1 > \widetilde{R}_1 > R_2$	$R_1 > \widetilde{R}_1 > R_2$
		$R_A > 1$	$R_A > 1$
E_A	$R_A > 1$	$R_A > R_1$	$R_A > \widetilde{\widetilde{R}}_1 > R_1$
		$R_A > \widetilde{R}_A > R_2$	$R_A > \widetilde{R}_A > R_2$
		$R_2 > 1$	$R_2 > 1$
E_2	$R_2 > 1$	$R_2 > R_1$	$R_2 > \widetilde{\widetilde{R}}_1 > R_1$
		$R_2 > R_A$	$R_2 > \widetilde{\widetilde{R}}_A > R_A$
$\bar{E}$	$\widetilde{R}_1 < R_2 < R_1$	$\widetilde{R}_1 < R_2 < R_1$	$\widetilde{R}_1 < R_2 < R_1$
		$R_1 > R_A$	condition (4.3)
$\hat{E}$	$\widetilde{R}_A < R_2 < R_A$	$\widetilde{R}_A < R_2 < R_A$	$\widetilde{R}_A < R_2 < R_A$
		$R_A > R_1$	condition (4.3)

ADE poses a significant risk to vaccine safety. Beyond influenza, ADE has been well established in viruses with multiple serotypes, most notably dengue, and remains a theoretical concern for other pathogens, including SARS-CoV-2. Accurately quantifying the impact of ADE risk on vaccination strategies presents complex multiobjective trade-offs and computational challenges in dynamic optimization. To address this, we developed a two-strain optimal control model for vaccination that explicitly integrates the ADE risk. Our analysis systematically reveals a quantifiable trade-off between risk aversion and epidemic control efficacy—an aspect not fully addressed in prior ADE-prone multistrain epidemic models—and identifies an optimal risk aversion interval that balances safety with effectiveness. The proposed framework not only provides a scientific foundation for decision-making in dual-strain vaccination campaigns but is also readily adaptable to complex public health scenarios, such as emergency vaccination during outbreaks of emerging infectious diseases. It thus offers a generalizable methodology for optimizing the balance between safety and efficacy in the face of uncertainty.

Use of AI tools declaration

The authors declare they have not used Artificial Intelligence (AI) tools in the creation of this article.

Acknowledgments

The work is supported by the Natural Science Foundation of Shaanxi Province Project (2023-JC-YB-084).

Conflict of interest

The authors declare there are no conflicts of interest.

References

1. Z. T. Xu, L. C. Qu, Y. H. Huang, Global dynamics of a two-strain flu model with delay, *Math. Comput. Simul.*, **124** (2016), 44–59. https://doi.org/10.1016/j.matcom.2015.10.016
2. Y. Chen, J. P. Zhang, Z. Jin, Optimal control of an influenza model with mixed cross-infection by age group, *Math. Comput. Simul.*, **206** (2023), 410–436. https://doi.org/10.1016/j.matcom.2022.11.019
3. M. A. Alshaikh, Stability of discrete-time delayed influenza model with two-strain and two vaccinations, *Results Phys.*, **28** (2021), 104563. https://doi.org/10.1016/j.rinp.2021.104563
4. WHO, Western Pacific. Available from: https://www.who.int/westernpacific/.
5. Z. W. Chen, Z. T. Xu, A delayed diffusive influenza model with two-strain and two vaccinations, *Appl. Math. Comput.*, **349** (2019), 439–453. https://doi.org/10.1016/j.amc.2018.12.065
6. A. J. N. May, E. J. A. Vales, Global dynamics of a two-strain flu model with a single vaccination and general incidence rate, *Math. Biosci. Eng.*, **17** (2020), 7862–7891. https://doi.org/10.3934/mbe.2020400
7. X. Y. Zheng, Q. Q. Chen, M. C. Sun, Q. Zhou, H. H. Shi, X. Y. Zhang, et al., Exploring the influence of environmental indicators and forecasting influenza incidence using ARIMAX models, *Front. Public Health*, **12** (2024), 1441240. https://doi.org/10.3389/fpubh.2024.1441240
8. M. Saade, S. Ghosh, M. Banerjee, V. Volpert, Dynamics of delay epidemic model with periodic transmission rate, *Appl. Math. Modell.*, **138** (2025), 115802. https://doi.org/10.1016/j.apm.2024.115802
9. R. Kulkarni, Antibody-dependent enhancement of viral infections, in *Dynamics of Immune Activation in Viral Diseases*, Springer, (2019), 9–41. https://doi.org/10.1007/978-981-15-1045-8_2
10. R. Narayan, S. Tripathi, Intrinsic ADE: the dark side of antibody dependent enhancement during dengue infection, *Front. Cell. Infect. Microbiol.*, **10** (2020), 580096. https://doi.org/10.3389/fcimb.2020.580096
11. M. C. Gómez, H. M. Yang, A simple mathematical model to describe antibody-dependent enhancement in heterologous secondary infection in dengue, *Math. Med. Biol.*, **36** (2019), 411–438. https://doi.org/10.1093/imammb/dqy016

12. F. de A. Camargo, M. Adimy, L. Esteva, C. Métayer, C. P. Ferreira, Modeling the relationship between antibody-dependent enhancement and disease severity in secondary dengue infection, *Bull. Math. Biol.*, **83** (2021), 85. https://doi.org/10.1007/s11538-021-00919-y

13. L. Billings, A. Fiorillo, I. B. Schwartz, Vaccinations in disease models with antibody-dependent enhancement, *Math. Biosci.*, **211** (2008), 265–281. https://doi.org/10.1016/j.mbs.2007.08.004

14. H. T. Song, Z. P. Yuan, S. Q. Liu, Z. Jin, G. Q. Sun, Mathematical modeling the dynamics of SARS-CoV-2 infection with antibody-dependent enhancement, *Nonlinear Dyn.*, **111** (2023), 2943–2958. https://doi.org/10.1007/s11071-022-07939-w

15. L. P. Wang, H. Y. Zhao, Dynamics analysis of a Zika–dengue co-infection model with dengue vaccine and antibody-dependent enhancement, *Physica A*, **522** (2019), 248–273. https://doi.org/10.1016/j.physa.2019.01.099

16. M. K. Smatti, A. A. Al Thani, H. M. Yassine, Viral-induced enhanced disease illness, *Front. Microbiol.*, **9** (2018), 2991. https://doi.org/10.3389/fmicb.2018.02991

17. WHO, Influenza (seasonal). Available from: https://www.who.int/news-room/fact-sheets/detail/influenza-(seasonal).

18. M. B. Moussa, A. Nwosu, K. Schmidt, S. Buckrell, A. Rahal, L. Lee, et al., National Influenza Annual Report 2023–2024: A focus on influenza B and public health implications, *Can. Commun. Dis. Rep.*, **50** (2024), 393–399. https://doi.org/10.14745/ccdr.v50i11a03

19. P. Van den Driessche, J. Watmough, Reproduction numbers and sub-threshold endemic equilibria for compartmental models of disease transmission, *Math. Biosci.*, **180** (2002), 29–48. https://doi.org/10.1016/S0025-5564(02)00108-6

20. J. P. LaSalle, *The Stability of Dynamical Systems*, SIAM, Philadelphia, PA, 1976. https://doi.org/10.1137/1.9781611970432

21. M. Y. Li, J. S. Muldowney, A geometric approach to global-stability problems, *SIAM J. Math. Anal.*, **27** (1996), 1070–1083. https://doi.org/10.1137/S0036141094266449

22. X. M. Feng, S. G. Ruan, Z. D. Teng, K. Wang, Stability and backward bifurcation in a malaria transmission model with applications to the control of malaria in China, *Math. Biosci.*, **266** (2015), 52–64. https://doi.org/10.1016/j.mbs.2015.05.005

23. H. I. Freedman, S. Ruan, M. Tang, Uniform persistence and flows near a closed positively invariant set, *J. Dyn. Differ. Equations*, **6** (1994), 583–600. https://doi.org/10.1007/BF02218848

24. V. Hutson, K. Schmitt, Permanence and the dynamics of biological systems, *Math. Biosci.*, **111** (1992), 1–71. https://doi.org/10.1016/0025-5564(92)90078-B

25. R. H. Martin, Logarithmic norms and projections applied to linear differential systems, *J. Math. Anal. Appl.*, **45** (1974), 432–454. https://doi.org/10.1016/0022-247X(74)90084-5

26. C. E. Ammon, Spanish flu epidemic in 1918 in Geneva, Switzerland, *Eurosurveillance*, **7** (2002), 190–192. https://doi.org/10.2807/esm.07.12.00391-en

27. Y. L. Chen, F. Tang, Z. C. Cao, J. F. Zeng, Z. K. Qiu, C. Zhang, et al., Global pattern and determinant for interaction of seasonal influenza viruses, *J. Infect. Public Health*, **17** (2024), 1086–1094. https://doi.org/10.1016/j.jiph.2024.04.024

28. D. Rios-Doria, G. Chowell, Qualitative analysis of the level of cross-protection between epidemic waves of the 1918–1919 influenza pandemic, *J. Theor. Biol.*, **261** (2009), 584–592. https://doi.org/10.1016/j.jtbi.2009.08.020
29. M. Sadki, K. Allali, Stochastic two-strain epidemic model with bilinear and non-monotonic incidence rates, *Eur. Phys. J. Plus*, **138** (2023), 923. https://doi.org/10.1140/epjp/s13360-023-04563-4
30. J. Y. Yang, L. Yang, L. Xue, Optimal control of a multi-scale immuno-influenza A transmission model with viral load-dependent infection, *Appl. Math. Modell.*, **132** (2024), 1–21. https://doi.org/10.1016/j.apm.2024.04.036
31. L. H. Zhou, M. Fan, Q. Hou, Z. Jin, X. D. Sun, Transmission dynamics and optimal control of brucellosis in Inner Mongolia of China, *Math. Biosci. Eng.*, **15** (2017), 543–567. https://doi.org/10.3934/mbe.2018025
32. Y. Li, L. W. Wang, L. Y. Pang, S. H. Liu, The data fitting and optimal control of a hand, foot and mouth disease (HFMD) model with stage structure, *Appl. Math. Comput.*, **276** (2016), 61–74. https://doi.org/10.1016/j.amc.2015.11.090
33. Y. Y. Dan, P. A. Tambyah, J. Sim, J. Lim, L. Y. Hsu, W. L. Chow, et al., Cost-effectiveness analysis of hospital infection control response to an epidemic respiratory virus threat, *Emerg. Infect. Dis.*, **15** (2009), 1909. https://doi.org/10.3201/eid1512.090902
34. P. Doyon-Plourde, J. Przepiorkowski, K. Young, L. Zhao, A. Sinilaite, Intraseasonal waning immunity of seasonal influenza vaccine: a systematic review and meta-analysis, *Vaccine*, **41** (2023), 4462–4471. https://doi.org/10.1016/j.vaccine.2023.06.038

Appendix

A. Block entries of the matrix Q

This appendix provides the complete block entries of the matrix $Q(s, i_1, i_A, r_1, i_2) = P_f P^{-1} + PJ^{[2]}P^{-1}$, which is used in the geometric approach to prove the global asymptotic stability of the endemic equilibrium $\bar{E}$ (Theorem 4.6).

$$Q_{11} = M_1 - \frac{i_1'}{i_1},\ Q_{12} = (0,0),\ Q_{13} = (0,\beta_A s),\ Q_{14} = (0,(1+\phi_1)\beta_2 s),\ Q_{15} = (0,0),\ Q_{16} = 0,$$

$$Q_{21} = (0,\eta_1)^{\mathrm{T}},\ Q_{22} = \begin{pmatrix} M_2 - \frac{i_1'}{i_1} & 0 \\ \eta_A & M_3 - \frac{i_1'}{i_1} \end{pmatrix},\ Q_{23} = \begin{pmatrix} 0 & -\beta_1 s \\ -\phi_2\beta_2 r_1 & 0 \end{pmatrix},\ Q_{24} = \begin{pmatrix} 0 & 0 \\ -\beta_1 s & 0 \end{pmatrix},$$

$$Q_{25} = \begin{pmatrix} 0 & (1+\phi_1)\beta_2 s \\ -\beta_A s & 0 \end{pmatrix},\ Q_{26} = (0,(1+\phi_1)\beta_2 s)^{\mathrm{T}},\ Q_{31} = (0,-\beta_A i_A)^{\mathrm{T}},\ Q_{32} = \begin{pmatrix} 0 & \phi_2\beta_2 i_2 \\ \beta_1 i_1 & 0 \end{pmatrix},$$

$$Q_{33} = \begin{pmatrix} M_4 - \frac{i_A'}{i_A} & 0 \\ 0 & M_5 - \frac{i_A'}{i_A} \end{pmatrix},\ Q_{34} = \begin{pmatrix} 0 & -\beta_1 s \\ 0 & 0 \end{pmatrix},\ Q_{35} = \begin{pmatrix} 0 & -\beta_A s \\ 0 & 0 \end{pmatrix},\ Q_{36} = (0,0)^{\mathrm{T}},$$

$$Q_{41} = (0,-(1+\phi_1)\beta_2 i_2)^{\mathrm{T}},\ Q_{42} = \begin{pmatrix} 0 & \beta_1 i_1 \\ 0 & 0 \end{pmatrix},\ Q_{43} = \begin{pmatrix} 0 & \eta_A \\ \beta_1 i_1 & 0 \end{pmatrix},\ Q_{44} = \begin{pmatrix} M_6 - \frac{i_A'}{i_A} & -\phi_2\beta_2 r_1 \\ \phi_2\beta_2 i_2 & M_7 - \frac{i_A'}{i_A} \end{pmatrix},$$

$$Q_{45} = \begin{pmatrix} 0 & 0 \\ 0 & 0 \end{pmatrix},\ Q_{46} = (0,0)^{\mathrm{T}},\ Q_{51} = (0,0)^{\mathrm{T}},\ Q_{52} = \begin{pmatrix} 0 & \beta_A i_A \\ -(1+\phi_1)\beta_2 i_2 & 0 \end{pmatrix},\ Q_{53} = \begin{pmatrix} 0 & -\eta_1 \\ \beta_A i_A & 0 \end{pmatrix},$$

$$Q_{54} = \begin{pmatrix} 0 & 0 \\ 0 & 0 \end{pmatrix},\ Q_{55} = \begin{pmatrix} M_8 - \frac{i_2'}{i_2} & -\phi_2\beta_2 r_1 \\ \phi_2\beta_2 i_2 & M_9 - \frac{i_2'}{i_2} \end{pmatrix},\ Q_{56} = (0,0)^{\mathrm{T}},\ Q_{61} = 0,\ Q_{62} = (0, -(1+\phi_1)\beta_2 i_2),$$

$$Q_{63} = (0,0),\ Q_{64} = (0,\eta_1),\ Q_{65} = (0,\eta_A),\ Q_{66} = M_{10} - \frac{i_2'}{i_2}.$$

B. Sensitivity analysis of ADE factors and model simplification

To assess the relative importance of exogenous (ϕ_1) and endogenous (ϕ_2) ADE effects on key model outputs, we performed a normalized sensitivity index (NSI) analysis. The NSI is defined as $S_\phi^Y = \frac{\partial Y}{\partial \phi} \cdot \frac{\phi}{Y}$, which measures the percentage change in output Y resulting from a 1% change in parameter ϕ around the baseline value ($\phi_1 = \phi_2 = 1.13$, estimated from the 1918 Geneva influenza data). Following standard conventions, $|S| > 1$ indicates high sensitivity, $0.2 < |S| \leq 1$ indicates moderate sensitivity, and $|S| \leq 0.2$ indicates low or negligible sensitivity.

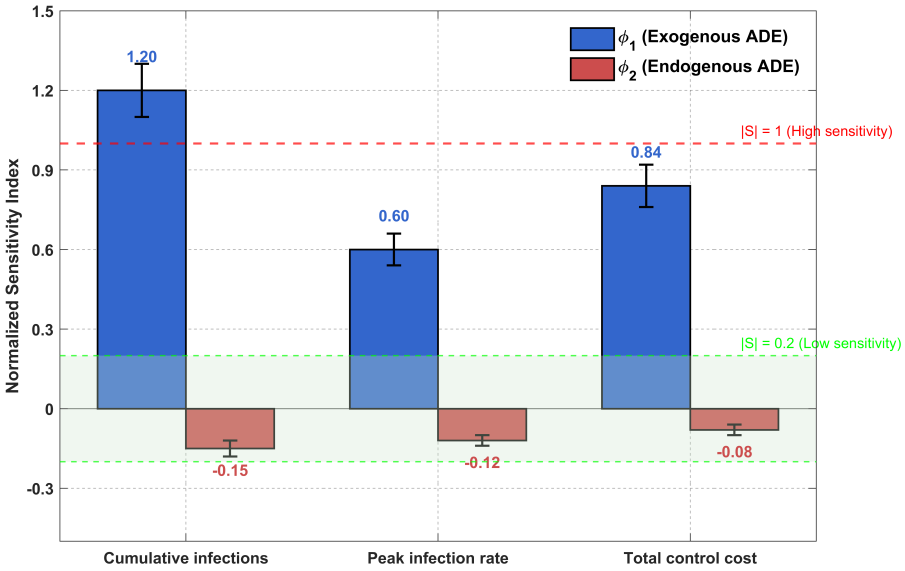

Figure B1. Sensitivity of ADE factors on key model outputs.

Figure B1 presents the NSI results for three key outputs: Cumulative infections, peak infection rate, and total optimal control cost. The analysis reveals a clear asymmetry between the two ADE mechanisms. Specifically, ϕ_1 exhibits high sensitivity for cumulative infections ($S = 1.20$), moderate sensitivity for peak infection rate ($S = 0.60$), and moderate sensitivity for the total control cost ($S = 0.84$). In contrast, ϕ_2 shows negligible sensitivity for all three outputs, with $|S| < 0.2$ in each case.

These results provide strong justification for the simplification $\phi_1 = \phi_2 = \phi$ adopted in our numerical simulations and optimal control analysis. Because ϕ_2 is insensitive for the key outputs of interest, any uncertainty or misspecification in ϕ_2 does not materially affect the model's main conclusions. Under the combined parameter ϕ, the model primarily captures the sensitive effects of exogenous ADE, ensuring

that the simplified framework remains robust and reliable for evaluating epidemic control strategies under ADE risk.

C. Complete adjoint equations

This appendix provides the complete adjoint equations used in the optimal control problem (Theorem 6.1). The adjoint variables λ_s, λ_{i_1}, λ_{i_A}, λ_{r_1}, λ_{i_2}, and λ_{r_2} satisfy the following system of differential equations, derived from $\frac{\partial H}{\partial x} = -\lambda_x'$ (where x denotes each state variable):

$$
\begin{aligned}
\lambda_s' &= -\frac{\partial H}{\partial s} \\
&= -2\omega_3 B_3^2 u_3^2(t)s(t) - 2\omega_4 B_4^2 s(t)(u_4^2(t) + u_5^2(t)) + \mu\lambda_s + (1 - u_3(t) - u_4(t))[\beta_1 i_1(\lambda_s - \lambda_{i_1}) \\
&\quad + \beta_A i_A(\lambda_s - \lambda_{i_A})] + (1 - u_3(t) - u_5(t))(1 + \phi)\beta_2 i_2(\lambda_s - \lambda_{i_2}), \\
\lambda_{i_1}' &= -\frac{\partial H}{\partial i_1} \\
&= -2\omega_1 B_1^2 u_1^2(t)(i_1(t) + i_A(t)) - 2\omega_5 D_1^2(i_1(t) + i_A(t)) - \alpha + \mu\lambda_{i_1} + (1 - u_3(t) - u_4(t))\beta_1 s(\lambda_s - \lambda_{i_1}) \\
&\quad + (1 + u_1(t))\eta_1(\lambda_{i_1} - \lambda_{r_1}), \\
\lambda_{i_A}' &= -\frac{\partial H}{\partial i_A} \\
&= -2\omega_1 B_1^2 u_1^2(t)(i_1(t) + i_A(t)) - 2\omega_5 D_1^2(i_1(t) + i_A(t)) + \mu\lambda_{i_A} + (1 - u_3(t) - u_4(t))\beta_A s(\lambda_s - \lambda_{i_A}) \\
&\quad + \eta_A(\lambda_{i_A} - \lambda_{r_1}), \\
\lambda_{r_1}' &= -\frac{\partial H}{\partial r_1} = -0.2\alpha + \mu\lambda_{r_1} + (1 - u_3(t) - u_5(t))\phi\beta_2 i_2(\lambda_{r_1} - \lambda_{i_2}), \\
\lambda_{i_2}' &= -\frac{\partial H}{\partial i_2} \\
&= -2\omega_2 B_2^2 u_2^2(t) i_2(t) - 2\omega_5 D_2^2 i_2(t) - 3\alpha + \mu\lambda_{i_2} + (1 - u_3(t) - u_5(t))[(1 + \phi)\beta_2 s(\lambda_s - \lambda_{i_2}) \\
&\quad + \phi\beta_2 r_1(\lambda_{r_1} - \lambda_{i_2})] + (1 + u_2(t))\eta_2(\lambda_{i_2} - \lambda_{r_2}), \\
\lambda_{r_2}' &= -\frac{\partial H}{\partial r_2} = \mu\lambda_{r_2}.
\end{aligned}
$$